

000 SEMANTIC F1 SCORES: FAIR EVALUATION 001 UNDER FUZZY CLASS BOUNDARIES 002

003 **Anonymous authors**
004

005 Paper under double-blind review
006

007 ABSTRACT 008

009 We propose **Semantic F1 Scores**, novel evaluation metrics for subjective or fuzzy
010 multi-label classification that quantify semantic relatedness between predicted and
011 gold labels. Unlike the conventional F1 metrics that treat semantically related pre-
012 dictions as complete failures, Semantic F1 incorporates a label similarity matrix
013 to compute soft precision-like and recall-like scores, from which the Semantic
014 F1 scores are derived. Unlike existing similarity-based metrics, our novel two-
015 step precision-recall formulation enables the comparison of label sets of arbitrary
016 sizes without discarding labels or forcing matches between dissimilar labels. By
017 granting partial credit for semantically related but nonidentical labels, Semantic
018 F1 better reflects the realities of domains marked by human disagreement or fuzzy
019 category boundaries. In this way, it provides fairer evaluations: it recognizes that
020 categories overlap, that annotators disagree, and that downstream decisions based
021 on similar predictions lead to similar outcomes. Through theoretical justification
022 and extensive empirical validation on synthetic and real data, we show that Se-
023 mantic F1 demonstrates greater interpretability and ecological validity. Because it
024 requires only a domain-appropriate similarity matrix, which is robust to misspec-
025 ification, and not a rigid ontology, it is applicable across tasks and modalities.
026

027 1 INTRODUCTION 028

029 Multi-label classification in subjective or conceptually rich domains, like emotion recognition or
030 identifying expressions of moral foundations, frequently involves labels that are semantically inter-
031 related or even interchangeable in some settings. Standard evaluation metrics such as F1 scores (Fu-
032 jino et al., 2008; Loza Mencía et al., 2023) treat any inexact match as a complete failure, even when
033 the predicted label is close to the “gold” label (e.g., *anger* and *disgust*). In practice, researchers
034 and practitioners routinely apply hard evaluation metrics to subjective classification tasks because
035 they represent the current standard and are compatible with existing evaluation pipelines (Alhuzali
036 & Ananiadou, 2021; Chochlakis et al., 2023a; Sabour et al., 2024; Lian et al., 2025). Crucially, in
037 these domains there is often no single “correct” answer or objective “ground truth”. It is typically
038 substituted with “crowd” truth (Aroyo & Welty, 2015; Resnick et al., 2021), relying on the wisdom
039 of the crowd. Disagreement is the norm, and errors are also common (Chochlakis et al., 2025).
040

041 To address these issues, we introduce **Semantic F1**, a family of metrics that extends the standard F1
042 measure by granting partial credit proportional to the semantic similarity between predicted and gold
043 labels in multi-label settings, which yields a label similarity matrix. Given such a label similarity
044 matrix, we then compute a two-step match: (i) map each prediction to its closest gold label (semantic
045 precision), (ii) map each gold label to its closest prediction (semantic recall). We next combine them
046 via harmonic mean, mirroring classic F1, to derive **sample**, **micro**, and **macro Semantic F1 scores**.
047 This two-step process is also shown in Figure 1 (and in 8 for a hierarchical label tree). Our novel
048 two-step design avoids common pitfalls of previous single-step algorithms (Kuhn, 1955; Sun & Lim,
049 2001; Turki et al., 2020) for semantic evaluation metrics, as it accounts for both **over-prediction**
050 (semantically unrelated predictions) and **under-coverage** (missing label coverage) of the semantic
051 label space. Importantly, Semantic F1 is grounded in existing evaluation theory. In the special case
052 where no partial credit is desired, Semantic F1 scores reduce exactly to the conventional F1 scores.
053

Beyond the theoretical framing, we validate Semantic F1 across eight synthetic and real-data studies.
We show that hard F1 fails to separate provably worse predictors, whereas Semantic F1 decays lin-

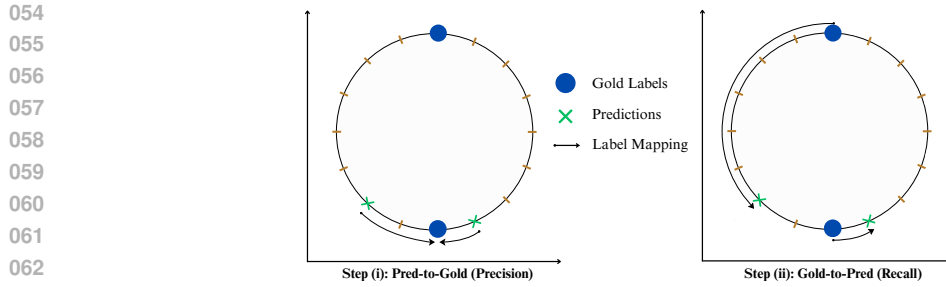


Figure 1: Qualitative demonstration of the matching method used between two sets of labels. Each prediction is mapped to its closest gold label, and vice versa, capturing **over-prediction** and **under-coverage** respectively. For visualization purposes, labels are placed on a unit circle, in a metric space where distance is measured based on angles, similar to (Plutchik, 1980)’s wheel of emotions.

early with both error rate and magnitude, remains robust to partial misspecification of the similarity matrix, and operates successfully in non-metric spaces by capturing cross-manifold errors. Notably, it avoids failure modes of existing semantic metrics. We also test LLMs on subjective tasks including predicting emotions (metric), moral foundations (non-metric), and downstream negotiation outcomes. Semantic F1 better reflects model performance, correlates more strongly with downstream outcomes, and behaves more intuitively under varying thresholds. Finally, using Semantic F1 for early stopping consistently yields superior generalization across both hard and semantic metrics.

Semantic F1 is built for practical deployment. It supports the common case of discrete label predictions and requires only a similarity matrix, which can be precomputed from domain knowledge, correlations, or embeddings. Unlike regression-based similarity measures, it naturally compares sets of *arbitrary* size, making it directly applicable to multi-label regression as well.

Our contributions can be summarized as follows: we introduce a novel suite of metrics, Semantic F1 scores, that leverage semantic relatedness to evaluate predictors. We show that our 2-step formulation is interpretable and has intuitive theoretical properties and no failure modes, compared to previous work. We also mathematically show that Semantic F1 scores fallback to the conventional F1 scores when no partial credit is assigned, providing extra guarantees of robustness. We conduct extensive experiments to validate the utility of the proposed metrics compared to existing work.

2 RELATED WORK

2.1 ONTOLOGY-DRIVEN SEMANTIC EVALUATION

Turki et al. (2020) proposed constructing confusion matrices that align predicted and gold labels using ontology-driven similarity, thereby enabling semantically weighted evaluation in multi-label settings. While this approach awards partial credit, it relies on a single alignment direction and conditions on the relative size of the two sets. As a result, it fails to penalize both over-prediction and under-coverage symmetrically, producing biased or incomplete assessments. Bansal et al. (2022) proposed a similar algorithm, but aimed at single-label sentence retrieval. An alternative is the Hungarian algorithm (Kuhn, 1955), which enforces one-to-one matches between predictions and gold labels. This constraint often discards legitimate predictions or gold labels, leading to unintuitive penalties, and its natural extensions introduce additional failure modes. In contrast, our two-step formulation maps directly onto precision and recall, preserving the robustness guarantees of the F1 score, avoiding the above pitfalls. Thus, it subsumes Turki et al. (2020) and resolves the limitations of Hungarian-style and other single-step similarity-based algorithms, as discussed in §3.2. Hierarchical multi-label classification approaches use semantics, where matches can be extended to larger neighborhoods in a hierarchical tree (Sun & Lim, 2001; Amigo & Delgado, 2022).

2.2 COST-SENSITIVE MULTI-LABEL LEARNING

Bénédict et al. (2021) introduced sigmoidF1, a smooth and differentiable approximation of F1 that can be optimized during training. Similarly, Lin (2023) introduced probability-guided losses. Both

108 maintain exact matches between labels. Rossi et al. (2018) introduced SML, leveraging label similarity
 109 during model training. Alhuzali & Ananiadou (2021); Chochlakis et al. (2023a); Huang et al.
 110 (2024) used label relationships at the example level during training. He & Xia (2018); Chochlakis
 111 et al. (2023a) used the cosine similarity of emotional representations for regularization. Hierarchical
 112 multi-label learning has also used graph-based similarity (Ramírez-Corona et al., 2016; Amigo &
 113 Delgado, 2022). Semantic F1 score, in contrast to all these approaches, introduces an algorithm to
 114 holistically match sets of labels in multi-label settings, as opposed to the exact matches, even if soft.
 115

116 2.3 LABEL SIMILARITY

117 Efforts to model label similarity span theoretical, embedding-based, and metric learning approaches.
 118 In emotion research, labels are often embedded in psychological spaces such as Plutchik (1980)'s
 119 wheel of emotions or the Circumplex model by Russell (1980), sometimes extended with Domi-
 120 nance or higher-dimensional representations (Demszky et al., 2020). These spaces provide direct
 121 measures of similarity between emotions and are commonly applied in regression-based recognition
 122 for single-label settings, where the label space is assumed metric. By contrast, moral foundations
 123 exemplify *multiple, separable clusters*: classic Moral Foundations Theory distinguishes *binding*
 124 (Loyalty, Authority, Purity) from *individualizing* (Care, Fairness) foundations (Graham et al., 2009;
 125 2011), and recent work further splits Fairness into *Equality* and *Proportionality* (Atari et al., 2023).

126 Embedding methods have also been deployed. Word2vec (Mikolov et al., 2013) and GloVe (Pen-
 127 nnington et al., 2014) embeddings enable similarity-based classification (Alhuzali & Ananiadou,
 128 2021; Chochlakis et al., 2023a), even in zero-shot scenarios (Wang et al., 2018; Chochlakis et al.,
 129 2023b). More recently, metric-learning approaches have explicitly optimized similarity structure.
 130 LIMIC (Mao et al., 2023) learns both global and label-specific metrics, while LSMM (Mao et al.,
 131 2024) extends this to multiple local metrics informed by semantic or clustering partitions. Hier-
 132 archival approaches instead exploit the label graph itself, using structural relationships to define
 133 similarity (Sun & Lim, 2001; McFee et al., 2017; Falis et al., 2021; Amigo & Delgado, 2022).

134 Despite this progress, no prior work has developed a principled semantic match for the predicted
 135 and gold label sets while preserving the interpretability and robustness of the F1 score. Semantic F1
 136 fills this gap by integrating semantic structure without sacrificing theoretical soundness.
 137

138 3 SEMANTIC F1 SCORE

140 3.1 PROBLEM FORMULATION

142 Consider a multi-label classification problem where we have input samples $\mathbf{x} \sim P(\mathcal{X})$ from an input
 143 space \mathcal{X} , and each sample is associated with a set of labels $\mathbf{y} \subseteq \mathcal{L}$, where $\mathcal{L} = \{\ell_1, \ell_2, \dots, \ell_m\}$
 144 is the universe of possible labels. \mathbf{y} is a set because multi-label settings can include none, one, or
 145 multiple labels in no particular order. Given a dataset $\mathcal{D} = \{(\mathbf{x}_i, T_i)\}_{i=1}^n$ where $T_i \subseteq \mathcal{L}$ represents
 146 the ground truth label set for example i , a classifier predicts label sets $P_i \subseteq \mathcal{L}$ for each input \mathbf{x}_i .
 147 In many real-world scenarios, the ground truth labels T_i may be noisy, incomplete, or come from
 148 unreliable annotators. Moreover, traditional evaluation metrics (e.g., conventional F1) treat all label
 149 mismatches equally, failing to account for semantic relationships between labels. To address this,
 150 we introduce semantic relatedness through a semantic similarity matrix $\mathbf{S} \in [0, 1]^{|\mathcal{L}| \times |\mathcal{L}|}$, where
 151 S_{ab} quantifies the semantic similarity between labels ℓ_a and ℓ_b . This similarity can be derived from
 152 label co-occurrence statistics, embedding distances, domain-specific knowledge graphs, or by using
 153 theoretical work in the domain (see §B).

154 3.2 CORE ALGORITHMS

156 **Matching Function** Let $A, B \subseteq \mathcal{L}$. The fundamental building block is the best matching function
 157 that computes the average semantic similarity of label set A to B :

$$158 \text{BestMatch}(A, B, S) = \frac{1}{|A|} \sum_{a \in A} \max_{b \in B} S_{a,b}. \quad (1)$$

160 This function, asymmetric in A and B , finds the best semantic match in set B for each element in set
 161 A , then returns the arithmetic mean of these maximum similarities. For all $a \in A$, we denote their

best match in B as $M_{A,B}(a)$. Intuitively, this matching function awards partial credit for semantic proximity in the space defined by S rather than treating all mismatches as zero, identifying how well the space occupied by A is semantically covered by B . Its time complexity is $O(|\mathcal{L}|^2)$, a small cost for most scenarios. We expand in §3.6 on how this runtime can be reduced, if required.

Pointwise Semantic F1 Score For a single example with predicted set P_i and gold set T_i , we apply the matching function in both directions, from P_i to T_i , and from T_i to P_i . Matching predictions to gold labels corresponds to what we define as **Semantic Precision**, as it quantifies how close the predictions are to some positive class in the semantic label space and, therefore, ignoring false negatives. As a result, it penalizes **over-prediction** in the label space, the semantic equivalent of false positives. On the other hand, matching gold labels to predictions corresponds to a **Semantic Recall**, quantifying how well gold label semantics are captured by some prediction in label space, while ignoring false positives. This is the semantic equivalent of capturing false negatives, which we refer to as **under-coverage**. Pointwise Semantic Precision, Recall, and F1 are defined as:

$$\text{Precision}_i^s = \text{BestMatch}(P_i, T_i, S), \quad (2)$$

$$\text{Recall}_i^s = \text{BestMatch}(T_i, P_i, S), \quad (3)$$

$$\text{SeF1}_i = H(\text{Precision}_i^s, \text{Recall}_i^s) = \frac{2 \cdot \text{Precision}_i^s \cdot \text{Recall}_i^s}{\text{Precision}_i^s + \text{Recall}_i^s}. \quad (4)$$

This is necessary to ensure that both **over-prediction** and **under-coverage** are penalized. Figure 1 also qualitatively demonstrates why both directions are essential in multi-label settings. In Figure 1(i), one gold label is unmatched; ignoring it would ignore under-coverage. Conversely, by flipping predictions and gold labels in Figure 1, the recall step only would leave one prediction unmatched, ignoring over-prediction. Alternatively, we could match all labels within a single step. A single step, however, does not have the interpretability of separate precision and recall steps, and it has to *force* unrelated matches, which intuitively is an undesirable property. We further elaborate on this and other theoretical limitations of existing single-step similarity-based approaches in §A.

3.3 SAMPLE SEMANTIC F1 SCORE

The sample Semantic F1 score is defined as the arithmetic mean of the pointwise scores:

$$\text{SeF1}_{\text{samples}} = \frac{1}{n} \sum_{i=1}^n \text{SeF1}_i. \quad (5)$$

A key edge case occurs when the similarity matrix is equal to the identity matrix $I_{|\mathcal{L}|}$ (denoted simply as I henceforth), and no partial credit is given to inexact predictions (this can happen, for example, when every label pair is distant in label space; we further discuss the interpretation of $S = I$ in §C). Then, we can easily derive that:

$$\text{BestMatch}(A, B, I) = \frac{|A \cap B|}{|A|} \Rightarrow \text{SeF1}_i = \frac{2 \cdot |P_i \cap T_i|}{|P_i| + |T_i|}, \quad (6)$$

making $\text{SeF1}_{\text{samples}}$ equivalent to the sample F1 score (Fujino et al., 2008; Loza Mencía et al., 2023) when $S = I$. Thus, the conventional (hard) sample F1 is a special case of our formulation. Likewise, without partial credit, semantic precision and recall also reduce to their conventional definitions.

3.4 MICRO SEMANTIC F1

The micro approach aggregates semantic relatedness across all examples before computing the F1 score. We define the semantic true positives, false positives, and false negatives as:

$$\text{TP}_i = \sum_{p \in P_i} S_{M_{P,T}(p), p} \Rightarrow \text{TP} = \sum_{i=1}^n \text{TP}_i \quad (7)$$

$$\text{FP}_i = \sum_{p \in P_i} (1 - S_{M_{P,T}(p), p}) \Rightarrow \text{FP} = \sum_{i=1}^n \text{FP}_i \quad (8)$$

$$\text{FN}_i = \sum_{t \in T_i} (1 - S_{t, M_{T,P}(t)}) \Rightarrow \text{FN} = \sum_{i=1}^n \text{FN}_i \quad (9)$$

216 Micro-averaged precision and recall are then computed in the usual way, yielding:
 217

$$218 \quad \text{SeF1}_{\text{micro}} = \frac{2 \cdot \text{TP}}{2 \cdot \text{TP} + \text{FP} + \text{FN}}. \quad (10)$$

220 As with the sample-based formulation, when $S = I$, the micro Semantic F1 reduces exactly to the
 221 conventional (hard) micro F1, and so do the micro Semantic Precision and Recall.
 222

223 3.5 MACRO SEMANTIC F1 224

225 For macro-averaging, we compute per-class Semantic F1 scores and average them. For each class
 226 $c \in \mathcal{L}$, we accumulate semantic counts across all examples in which it appears:
 227

$$228 \quad \text{TP}_c = \sum_{i=1}^n S_{M_{P,T}(c),c}, \quad \text{FP}_c = \sum_{i=1}^n 1 - S_{M_{P,T}(c),c}, \quad \text{FN}_c = \sum_{i=1}^n 1 - S_{c,M_{T,P}(c)} \quad (11)$$

230 The per-class and macro Semantic F1 scores are then defined as:
 231

$$232 \quad \text{SeF1}_c = \frac{2 \cdot \text{TP}_c}{2 \cdot \text{TP}_c + \text{FP}_c + \text{FN}_c} \Rightarrow \text{SeF1}_{\text{macro}} = \frac{1}{|\mathcal{L}|} \sum_{c \in \mathcal{L}} \text{SeF1}_c. \quad (12)$$

235 Again, setting $S = I$ collapses the macro Semantic F1 to the standard (hard) macro F1 score. We
 236 cover edge cases and other variants in §D, with pseudocode in §G.
 237

238 3.6 EXTENSION TO CONTINUOUS SPACES 239

240 So far, we have assumed fixed discrete gold and predicted labels, which permits the $O(|\mathcal{L}|^2)$ runtime
 241 and explicit precomputation of the similarity matrix. A key novelty of our approach is that it extends
 242 seamlessly to continuous semantic spaces without fixed label sets. This generalization not only
 243 broadens applicability but can also reduce runtime in the discrete case. Specifically, assuming $a, b \in$
 244 \mathbb{R}^d , the matching can be reformulated as

$$245 \quad \text{BestMatch}(A, B, D) = \frac{1}{|A|} \sum_{a \in A} \max_{b \in N(a, B)} \hat{S}(a, b; D), \quad (13)$$

247 where D is a distance measure (e.g., Euclidean for a metric space, Isomap (Tenenbaum et al., 2000)
 248 for a non-metric space) used to compute similarity \hat{S} online, such as $\hat{S}(a, b; \|\cdot\|_2) = \frac{1}{1 + \|a - b\|_2}$.
 249 N retrieves nearest neighbors of a in B , typically faster than brute-force $O(|B| \cdot d)$ search (Wang
 250 et al., 2024). This extension enables principled and interpretable evaluation in multidimensional
 251 multi-label regression and even classification, for instance when using prototypical embeddings (Pa-
 252 paioannou et al., 2025). Semantic F1 can then be computed as usual.
 253

254 4 EXPERIMENTS 255

256 4.1 DATASETS 257

258 **SemEval 2018 Task 1 E-c (Mohammad et al., 2018)** Subjective multi-label emotion recognition
 259 of 11 emotions. We use the English tweets. We refer to this as **SemEval** for short. Similarity is
 260 derived as normalized cosine similarity from Plutchik (1980)’s metric wheel.
 261

262 **GoEmotions (Demszky et al., 2020)** Subjective multi-label emotion recognition benchmark of
 263 27 emotions. Similarity is derived from train set correlations, which might not generalize to other
 264 settings due to the distinction between *semantic* and *associative* relations, which we discuss in §B.
 265

266 **MFRC (Trager et al., 2022)** Subjective multi-label moral foundation corpus from Reddit for six
 267 moral foundations. The majority of examples contains no labels, so similarity is derived from cor-
 268 relations in Atari et al. (2023). This dataset exemplifies a clustered, non-metric label space: classic
 269 Moral Foundations Theory distinguishes binding from individualizing foundations (Graham et al.,
 2009; 2011), with recent work further splitting them (Atari et al., 2023). As a result, MFRC provides
 a natural testbed for evaluating Semantic F1 in non-metric, multi-manifold domains where partial
 credit is meaningful within clusters but less so across them.

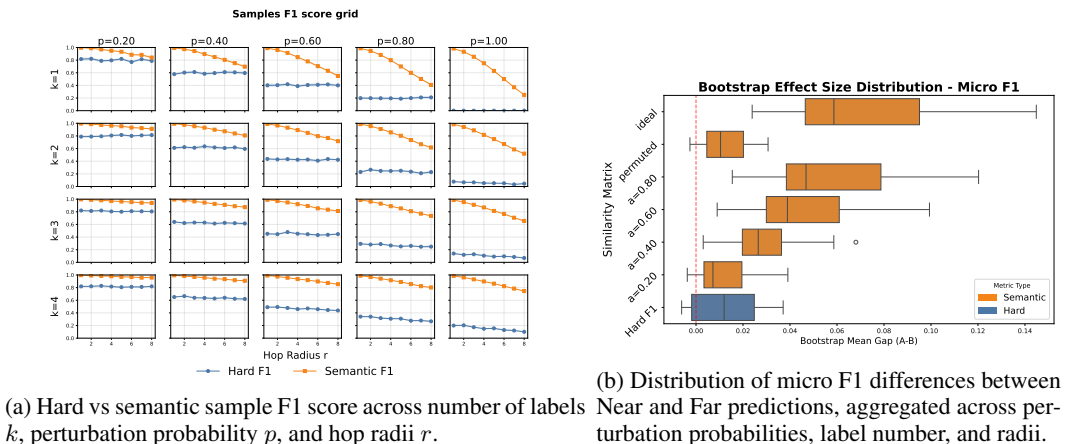
270 **PersuasionForGood (Wang et al., 2019)** Negotiation dialogues in which the persuader attempts
 271 to convince their interlocutor to donate part of their task earnings to charity. Donation amounts for
 272 persuader and persuadee are provided. We formulate a binary prediction task, *persuader success*,
 273 denoting whether the persuadee donates more than the persuader, evaluated using the ROC-AUC
 274 score. Because it does not include emotion annotations, we manually annotated two examples per
 275 taxonomy (GoEmotions or SemEval) for use in prompting. Emotions are then predicted per turn,
 276 given previous turns as context. We adopt an 85–15 train/test split. We refer to this as **P4G**.
 277

278 4.2 IMPLEMENTATION DETAILS

280 We use the 4-bit quantized versions of the open-source LLMs through the *vLLM* (Kwon
 281 et al., 2023), *HuggingFace* (Wolf et al., 2020) and *bitandbytes* interface for *Py-
 282 Torch*. We use GPT-4.1 (gpt-4.1-mini), GPT-4o (gpt-4o-mini), Llama-2
 283 7B and 70B (meta-llama/Llama-2-#b-chat-hf), and Llama-3 8B and 70B
 284 (meta-llama/Llama-3.-#B-Instruct). We set set temperature to 0. We use ran-
 285 dom retrieval of examples. We finetune BERT (bert-base-uncased; Devlin et al. 2018) using
 286 Demux (Chochlakis et al., 2023a). Standard splits are used if not specified. More details in §E.
 287

288 4.3 RESULTS

289 To substantiate the utility of our proposed metric, we present four synthetic-data and four real-data
 290 studies. They address two key questions: (i) do the theoretical advantages of Semantic F1 translate
 291 to actual improvements in controlled, synthetic settings over hard F1 and baseline semantic-based
 292 metrics? and, (ii) does it provide more meaningful evaluation than current practice on real-world
 293 tasks? We use the synthetic settings to precisely control the behavior (the amount of error) of the
 294 predictions, which allows us to make precise claims about the behavior of the metrics across prov-
 295 ably worse predictors. The real-world tasks verify our theoretical findings and our results from the
 296 synthetic experiments in practice, using real data to supplement our synthetic results. The intuition
 297 behind real-world tasks is that a more informative metric will correlate better with other interesting
 298 aspects of the model and the data, providing indeed a better automated evaluation of models.
 299



311 (a) Hard vs semantic sample F1 score across number of labels 312 Near and Far predictions, aggregated across per-
 312 k, perturbation probability p , and hop radii r . 313
 314 (b) Distribution of micro F1 differences between 315 Near and Far predictions, aggregated across per-
 315 turbation probabilities, label number, and radii.

316 Figure 2: Semantic metrics scale with worse predictors, even with moderately misspecified simi-
 317 larity matrix, in contrast to hard metrics.

318 4.3.1 SYNTHETIC STUDY A: SYNTHETIC CONSTRUCT VALIDITY

319 **Motivation.** We test whether Semantic F1 properly reflects the semantic closeness between gold
 320 labels and predictions in a controlled setting, namely labels placed on a ring in a 2D space (similar
 321 to Plutchik (1980)’s wheel, see the individual components in Figure 14). We also evaluate the
 322 robustness to different degrees of misspecification of the similarity matrix. To do so, we add random
 323 noise in the non-diagonal elements of the similarity matrix and check whether the semantic metrics
 324 still sufficiently differentiate between provably better and worse classifiers. This would indicate that

324 knowing only roughly the similarity between labels is sufficient for Semantic F1 to serve as a good
 325 evaluation metric.
 326

327 **Setup.** We arrange $n = 24$ labels on a unit circle at angles $\theta_i = 2\pi i/n$ and define the ground-truth
 328 similarity S via normalized cosine similarity $S(i, j) = 0.5 + \cos(\theta_i - \theta_j)/2 \in [0, 1]$. Gold sets
 329 are generated by sampling k labels per example from a cosine-peaked distribution around a random
 330 center. Concretely, we first sample one label uniformly at random, then sample the remaining $k-1$
 331 labels with probabilities proportional to their similarity to the first label. We construct two families
 332 of perturbed predictors: *Near-miss* and *Far-miss*. For each gold label and perturbation probability
 333 p , we substitute the label with one exactly r hops away on the ring: $r \in \{r_{\text{near}}\}$ for Near, $r \in$
 334 $\{r_{\text{far}}\} > r_{\text{near}}$ for Far. We sweep $k \in \{1, 2, 3, 4\}$, $p \in \{0, 0.2, 0.4, 0.6, 0.8, 1\}$, and hop radii
 335 $r_{\text{near}} \in \{1, 2, 3, 4\}$, $r_{\text{far}} \in \{5, 6, 7, 8\}$. To assess robustness to similarity matrix misspecification, we
 336 evaluate under: (i) ideal S , (ii) a row-permuted, invalid S , and (iii) mixtures $S_\alpha = \alpha S + (1 - \alpha)U$
 337 with $\alpha \in \{0.8, 0.6, 0.4, 0.2\}$, where U is Gaussian noise of 0.5 deviation.
 338

339 **Metrics and statistics.** We report hard F1 using `sklearn` and Semantic F1 (mi-
 340 cro/macro/samples). We show how these metrics vary across hop radii r and perturbation prob-
 341 abilities p with 1000 examples per configuration. For sensitivity to true difficulty, we compute
 342 Kendall’s τ between metric value and the true radius r (expect decreasing with r). For Near vs. Far
 343 comparisons, we bootstrap the mean gap (A–B) with $B = 25$ resamples for 95% CIs.
 344

345 **Results.** Figure 2a shows sample F1 as a function of the number of gold labels k , perturbation
 346 probability p , and hop radius r , with mean and 95% CIs from bootstrapping. Hard metrics re-
 347 main largely invariant to hop radius and may even increase as predictions become less semantically
 348 relevant, indicating sensitivity to noise rather than semantic closeness. By contrast, Semantic F1 de-
 349 creases monotonically with both hop radius and perturbation probability. Corresponding Kendall’s
 350 τ statistics are reported in Figure 11 of §F.1. For Near vs. Far comparisons, Figure 2b (micro
 351 F1) shows the distribution of metric differences between r_{near} and r_{far} . Semantic F1 provides much
 352 clearer separation than hard F1. Moreover, Semantic F1 is robust to moderate to high misspeci-
 353 fication: even mixtures with $\alpha = 0.2$ maintain separation comparable to that of the hard metric.
 354 However, when the similarity matrix is fully permuted, separation collapses, eliminating any advan-
 355 tage over hard F1. Other metrics and full experimental grids are presented in §F.1.
 356

357 4.3.2 SYNTHETIC STUDIES B-D

358 We present results for synthetic studies B through D in the appendix, §F.2, §F.3, and §F.4 respec-
 359 tively. Briefly, synthetic study B examines heuristic bimodal classifiers, showing that hard metrics
 360 favor such simple heuristics over near-miss classifiers, unlike Semantic F1. Synthetic study C in-
 361 vestigates non-metric spaces: hard F1 remains invariant to within- and across-manifold jumps, even
 362 when the latter should be penalized, whereas Semantic F1 captures this distinction, even under mod-
 363 erate misspecification. However, when similarity is naively constructed under metric assumptions,
 364 Semantic F1 also becomes insensitive to cross-manifold errors, highlighting the need for caution
 365 in non-metric settings. Finally, synthetic study D demonstrates beyond the theoretical arguments
 366 in §3.2 and §A that other similarity-based baselines fail to separate good from bad predictors. The
 367 failure cases of semantic precision and recall are similar to the ones of their conventional coun-
 368 terparts, justifying the switch to the Semantic F1 score as a generic evaluation metric in domains
 369 without special considerations. For this reason, we focus on the Semantic F1 score for the following
 370 real-data studies. It is important to note, however, the precision and recall might be more appro-
 371 priate for domains where under-coverage or over-prediction respectively are not important. The
 372 extended Hungarian algorithm conflates over-prediction and under-coverage, creating failure modes
 373 that Semantic F1 does not have, making its usage in generic or special domains hard to justify.
 374

375 4.3.3 REAL STUDY A: MULTI-LABEL THRESHOLD BEHAVIOR

376 **Motivation.** We test whether Semantic F1 varies more smoothly with decision thresholds and
 377 yields more stable model rankings than standard hard F1 when applied to supervised multilabel
 378 heads. This would indicate that Semantic F1 is more robust to threshold choice, making evaluations
 379 less sensitive to hyperparameter choice.

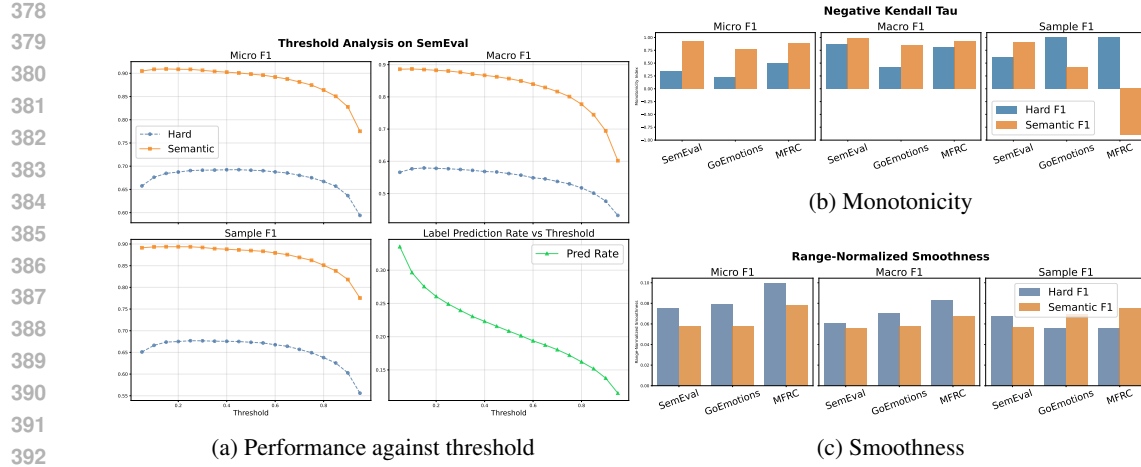


Figure 3: Threshold analysis on Demux

Setup. We evaluate multi-label classifiers, namely Demux and Llama-3 1B with trained classification head, on subjective multi-label datasets. For each dataset we fix a similarity matrix S , and for each model we sweep decision thresholds $\tau \in \{0.1, 0.2, \dots, 0.9\}$, binarize predictions and compute metrics at each τ .

Metrics and statistics. At every threshold we report hard F1 and Semantic F1 (micro/macro/samples). We summarize smoothness and ranking behavior across the threshold grid $\mathcal{T} = (\tau_1, \dots, \tau_T)$ with two indices: (i) Monotonicity: Kendall’s τ , reported as its negative value (so that more decreasing monotonic trends correspond to higher values, which we expect; thus, higher is better) (ii) Smoothness: the average absolute step change between consecutive thresholds, normalized by the value range (lower is better, since large jumps indicate “bumpiness”). Using absolute differences disentangles smoothness from monotonicity, while range normalization accounts for pragmatic scale differences between metrics. By convention, a higher monotonicity index and lower smoothness index indicate greater robustness to threshold choice.

Results. Figure 3 shows the threshold behavior of Demux on SemEval (with Llama-3 1B and full dataset results in §F.5). Semantic F1 declines more monotonically as thresholds increase, reflecting that lower probabilities often indicate semantically related but inexact labels, information captured by Semantic F1 but ignored by hard F1. Quantitative comparisons in Figure 3b and 3c show that across datasets and models, Semantic F1 consistently achieves a higher monotonicity index and lower smoothness index, demonstrating greater robustness to threshold variation and more stable model rankings than hard F1.

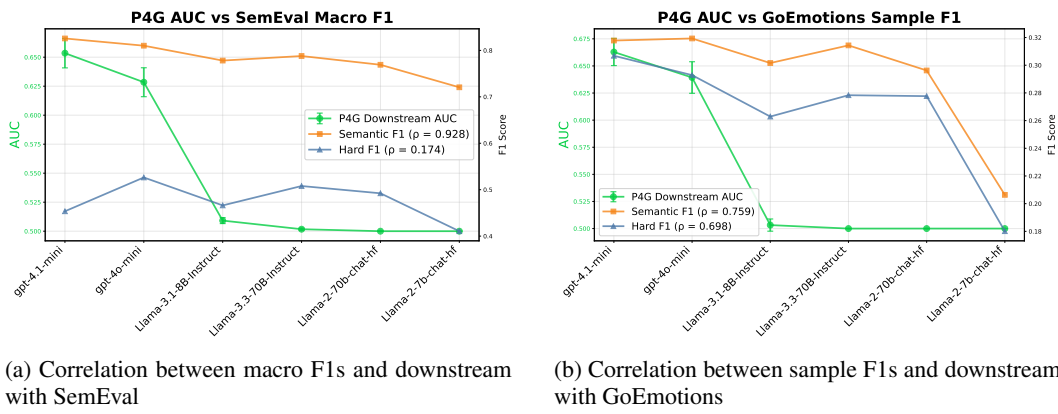
4.3.4 REAL STUDY B: ECOLOGICAL VALIDITY

Motivation. We test whether semantic similarity in subjective predictions matters for downstream applications. Specifically, we ask whether models ranked higher by Semantic F1 on subjective tasks produce emotional features that better predict outcomes in an objective downstream task than models ranked by conventional hard F1. Better correlation with downstream tasks signals a more informative and ecologically valid metric.

Setup. Using the SemEval and GoEmotions taxonomies, we predict emotions at every turn of negotiation dialogues with six LLMs, conditioned on prior turns. The predicted emotions are then used as features for logistic regression models that predict negotiation outcomes. Features are constructed by averaging predictions over the last k turns, and we report the best downstream performance across $k \in \{1, 2, \dots, 10\}$. Performance on the downstream task is compared to each model’s performance on the source emotion dataset (from which the taxonomy is drawn), using 2-shot prompts for both.

432 **Metrics and statistics.** We repeat each logistic or linear regression experiment with 100 different
 433 seeds and LLM inference 5 times for a subset of 300 test examples each to derive means and 95%
 434 confidence intervals. We report Spearman correlation between downstream performance and source-
 435 task performance across models.
 436

437 **Results.** Figure 4 shows that Semantic F1 correlates more strongly with downstream performance
 438 than hard F1. In particular, Figure 4a demonstrates that downstream outcomes are almost perfectly
 439 correlated with Semantic F1 (with $p < 0.01$), whereas correlation with hard F1 is absent. More
 440 broadly, across all settings (see §F.6), Semantic F1 is at least as predictive of downstream perfor-
 441 mance as hard F1. These findings highlight the ecological validity of Semantic F1: semantically
 442 similar, though not identical, emotion predictions yield quantitatively similar downstream effects,
 443 making Semantic F1 a better proxy for real-world utility. Notably, when using either only semantic
 444 precision or only semantic recall, that is not the case, as shown in §F.6.
 445



457 Figure 4: Ecological validity study results comparing semantic and hard F1 correlation with down-
 458 stream performance across different emotion datasets. X axis ordered by downstream performance.
 459

464 4.3.5 REAL STUDY C: EARLY STOPPING CRITERION

465 **Motivation.** We test whether Semantic F1 as early stopping criterion leads to better generalization
 466 than using hard F1 scores. The hypothesis is that predictors optimized for semantic similarity will
 467 generalize better, even if ultimately evaluated on hard matches.
 468

470 **Setup.** We train and evaluate Demux on SemEval, GoEmotions, and MFRC. We use either a hard
 471 F1 or a Semantic F1 metric as an early stopping criterion on the development set, and then evaluate
 472 the best model based on these on the test set.
 473

474 **Metrics and statistics.** We evaluate each model on seven metrics: Semantic and hard F1 (mi-
 475 cro/macro/samples; six in total) plus the Jaccard score. Each experiment is repeated 10 times, and
 476 we report means with 95% CIs. For comparisons between semantic-based and hard-based early
 477 stopping, we compute two-sided p-values testing equality of the resulting distributions.
 478

479 **Results.** Table 1 shows the number of metrics (development and test) on which runs using Sem-
 480 antic F1 for early stopping outperform those using hard F1, and vice versa. Semantic-based stopping
 481 consistently yields more favorable outcomes, both in terms of trends and statistically significant
 482 gains, compared to hard-based stopping. Particularly on MFRC, we see that with hard early stop-
 483 ping, only the criterion metric itself shows a significant improvement, while with semantic early
 484 stopping, gains extend even to Jaccard score, a purely hard metric. Full results across datasets are
 485 presented in §F.7. Overall, these findings indicate that semantic metrics provide superior early stop-
 486 ping criteria, producing models that generalize better across both semantic and hard metrics.
 487

486 Table 1: Early stopping method comparison: Wins across all metrics (6 F1s and Jaccard Score).
 487 Statistically significant wins are shown in parentheses. Early stopping criterion was sample F1.
 488

Dataset	Dev		Test	
	Semantic	Hard	Semantic	Hard
GoEmotions	7 (0)	0 (0)	2 (0)	5 (0)
MFRC	2 (2)	5 (0)	4 (2)	3 (1)
SemEval	4 (0)	3 (0)	7 (0)	0 (0)
Total	13 (2)	8 (0)	13 (2)	8 (1)

498 4.3.6 REAL STUDY D: CONVERGENT VALIDITY

500 We hypothesize that Semantic F1, when applied to subjective tasks, better reflects the performance
 501 improvements of newer LLMs on objective tasks than hard F1. As shown in §F.8, Semantic F1
 502 indeed tracks objective performance more faithfully: while Spearman correlations are comparable,
 503 its Concordance Correlation Coefficient (CCC) is substantially higher, indicating not only alignment
 504 in trends but also a much closer match in absolute values across a variety of similarity matrices.

506 5 CONCLUSION

509 We introduce the *Semantic F1* scores, a principled extension of the multi-label F1 score that incorpo-
 510 rates semantic similarity between labels while retaining the interpretability and robustness of preci-
 511 sion-recall reasoning. Our two-step formulation resolves the shortcomings of prior single-step and
 512 Hungarian-style approaches by penalizing both over-prediction and under-coverage without forcing
 513 spurious matches or discarding labels. Crucially, when no partial credit is assigned, Semantic
 514 F1 collapses exactly to standard F1, ensuring backward compatibility with existing pipelines, and
 515 extending the standard F1’s robustness to similarity-based metrics.

516 Through numerous studies, we demonstrate the advantages of Semantic F1. In controlled exper-
 517 iments, it scales smoothly with semantic error, distinguishes near- from far-miss predictors, and
 518 remains robust under moderate misspecification of the similarities, including in non-metric spaces.
 519 In real-world evaluations of LLMs, Semantic F1 produces more stable threshold behavior, stronger
 520 alignment with downstream outcomes, and improves generalization when used for early stopping.
 521 These findings establish Semantic F1 as both theoretically sound and practically effective.

522 One limitation of Semantic F1 lies in its dependence on the similarity matrix, as for any semantic
 523 metric. Although our experiments (§4.3, §F) show robustness to moderate misspecification and di-
 524 verse initializations, we recognize that poorly designed similarity matrices (e.g., dense, adversarial,
 525 or culturally inappropriate) may degrade interpretability or fairness, as we also show in §F.3. In
 526 practice, we recommend constructing similarity matrices from out-of-sample correlations, validated
 527 embeddings, or domain ontologies derived from work of domain experts, and inspecting their spar-
 528 sity and scaling before deployment, following §B and insights from §F.3 and §F.4. Future work
 529 could explore methods to further mitigate sensitivity. Importantly, when similarity reduces to the
 530 identity matrix, Semantic F1 gracefully collapses to standard F1, ensuring a safe fallback. Addition-
 531 ally, the framework should treat similarity matrices as culturally and contextually variable, rather
 532 than as universal structures (Atari et al., 2023).

533 Taken together, our synthetic and real-data results show that Semantic F1 provides a fairer and
 534 more informative evaluation for subjective and fuzzy classification tasks if appropriate semantic
 535 similarities between labels are used, offering a drop-in replacement for hard F1 that better reflects
 536 ecological validity and downstream utility. We believe that this metric fills a critical gap in evaluation
 537 methodology and can serve as a foundation for future work on semantically and culturally grounded
 538 subjective performance measures. We expect that each community will converge to a single or
 539 a fixed of similarity matrices to use for semantic evaluation, and urge dataset distributors to also
 release similarity matrices for their datasets as the canonical similarity to be used during evaluation,
 or clearly cite the theoretical work motivating their taxonomy.

540 ETHICS STATEMENT
541

542 Even when semantic similarity is properly captured, practitioners should *not* treat similarity judgments
543 as universal and should acknowledge their cultural and contextual variability. Different populations
544 demonstrate systematically different intuitions about semantic similarity: Atari et al. (2023),
545 where we derive our similarity matrix for morality, demonstrate so for moral foundations across
546 cultures, for example. Constant or sole reliance on established psychological models (e.g., Plutchik
547 (1980)'s wheel) or training correlations can hardcode one cultural perspective as universal, creating
548 systematic bias toward the population whose judgments the similarity matrix reflects. This limitation
549 is particularly problematic for AI systems deployed across diverse populations, where evaluation
550 fairness requires acknowledging that semantic relationships themselves are culturally constructed
551 rather than objectively given. Used properly, Semantic F1 can actually act as another measurement
552 tool for cultural bias, measuring preference for ontologies that emerge in specific cultures rather
553 than others.

554 Nevertheless, to address these limitations during evaluation, a methodological framework is needed
555 that treats similarity matrices as empirically validated, population-specific instruments rather than
556 fixed universal structures. This approach requires three components: (i) collecting human similarity
557 judgments from the target population through psychometric studies, e.g., where participants rate
558 label pairs on standardized scales, (ii) learning calibration functions that map embedding distances
559 to these human-derived similarity scores, and (iii) generating population-specific similarity matrices
560 that reflect the actual conceptual relationships meaningful to the intended user community. Once
561 validated, these calibration functions could be deployed beyond the original label set, in related
562 tasks for that same population.

563 REPRODUCIBILITY STATEMENT
564

565 We provide several resources to ensure clarity and reproducibility of our methods. Pseudocode for
566 all core algorithms is included in §G to avoid any ambiguity in implementation. Each study contains
567 dedicated **Setup** and **Metrics and statistics** sections, detailing experimental design and evaluation
568 to facilitate reproduction. In §B, we give explicit instructions for constructing similarity matrices,
569 and in §E we provide prompts and additional implementation details, complementing §4.2 in the
570 main text. Finally, we commit to releasing our code, including Semantic F1, baseline methods such
571 as the extended Hungarian, and all experimental pipelines, upon publication.

572
573 REFERENCES
574

575 Hassan Alhuzali and Sophia Ananiadou. Spanemo: Casting multi-label emotion classification as
576 span-prediction. *arXiv preprint arXiv:2101.10038*, 2021.

577 Enrique Amigo and Agustín Delgado. Evaluating extreme hierarchical multi-label classification. In
578 *Proceedings of the 60th Annual Meeting of the Association for Computational Linguistics (Volume
579 1: Long Papers)*, pp. 5809–5819, 2022.

580 Lora Aroyo and Chris Welty. Truth is a lie: Crowd truth and the seven myths of human annotation.
581 *AI Magazine*, 36(1):15–24, 2015.

582 Mohammad Atari, Jonathan Haidt, Jesse Graham, Sena Koleva, Sean T Stevens, and Morteza De-
583 hghani. Morality beyond the weird: How the nomological network of morality varies across
584 cultures. *Journal of Personality and Social Psychology*, 125(5):1157, 2023.

585 Naman Bansal, Mousumi Akter, and Shubhra Kanti Karmaker Santu. Sem-f1: an automatic way
586 for semantic evaluation of multi-narrative overlap summaries at scale. In *Proceedings of the 2022
587 Conference on Empirical Methods in Natural Language Processing*, pp. 780–792, 2022.

588 Gabriel Bénédict, Vincent Koops, Daan Odijk, and Maarten de Rijke. Sigmoidf1: A smooth f1 score
589 surrogate loss for multilabel classification. *arXiv preprint arXiv:2108.10566*, 2021.

590 Georgios Chochlakis, Gireesh Mahajan, Sabyasachee Baruah, Keith Burghardt, Kristina Lerman,
591 and Shrikanth Narayanan. Leveraging label correlations in a multi-label setting: A case study in

594 emotion. In *ICASSP 2023-2023 IEEE International Conference on Acoustics, Speech and Signal*
 595 *Processing (ICASSP)*, pp. 1–5. IEEE, 2023a. ISBN 1-7281-6327-7.

596

597 Georgios Chochlakis, Gireesh Mahajan, Sabyasachee Baruah, Keith Burghardt, Kristina Lerman,
 598 and Shrikanth Narayanan. Using Emotion Embeddings to Transfer Knowledge between Emo-
 599 tions, Languages, and Annotation Formats. In *ICASSP 2023-2023 IEEE International Conference*
 600 *on Acoustics, Speech and Signal Processing (ICASSP)*, pp. 1–5. IEEE, 2023b. ISBN 1-7281-
 601 6327-7.

602 Georgios Chochlakis, Peter Wu, Arjun Bedi, Marcus Ma, Kristina Lerman, and Shrikanth
 603 Narayanan. Humans hallucinate too: Language models identify and correct subjective annota-
 604 tion errors with label-in-a-haystack prompts. *arXiv preprint arXiv:2505.17222*, 2025.

605

606 Dorottya Demszky, Dana Movshovitz-Attias, Jeongwoo Ko, Alan Cowen, Gaurav Nemade, and
 607 Sujith Ravi. GoEmotions: A dataset of fine-grained emotions. In *Proceedings of the 58th Annual*
 608 *Meeting of the Association for Computational Linguistics*, pp. 4040–4054, 2020.

609 Jacob Devlin, Ming-Wei Chang, Kenton Lee, and Kristina Toutanova. Bert: Pre-training of deep
 610 bidirectional transformers for language understanding. *arXiv preprint arXiv:1810.04805*, 2018.

611

612 Matúš Falis, Hang Dong, Alexandra Birch, and Beatrice Alex. Cophe: A count-preserving
 613 hierarchical evaluation metric in large-scale multi-label text classification. *arXiv preprint*
 614 *arXiv:2109.04853*, 2021.

615

616 Akinori Fujino, Hideki Isozaki, and Jun Suzuki. Multi-label text categorization with model combina-
 617 tion based on f1-score maximization. In *Proceedings of the Third International Joint Conference*
 618 *on Natural Language Processing: Volume-II*, 2008.

619

620 Jesse Graham, Jonathan Haidt, and Brian A. Nosek. Liberals and conservatives rely on different sets
 621 of moral foundations. *Journal of Personality and Social Psychology*, 96(5):1029–1046, 2009.

622

623 Jesse Graham, Jonathan Haidt, Sena Koleva, et al. Mapping the moral domain. *Journal of Person-
 624 ality and Social Psychology*, 101(2):366–385, 2011.

625

626 F Maxwell Harper and Joseph A Konstan. The movielens datasets: History and context. *Acm*
 627 *transactions on interactive intelligent systems (tiis)*, 5(4):1–19, 2015.

628

629 Huihui He and Rui Xia. Joint binary neural network for multi-label learning with applications to
 630 emotion classification. In *CCF International Conference on Natural Language Processing and*
 631 *Chinese Computing*, pp. 250–259. Springer, 2018.

632

633 Eduard Hovy, Laurie Gerber, Ulf Hermjakob, Chin-Yew Lin, and Deepak Ravichandran. To-
 634 ward semantics-based answer pinpointing. In *Proceedings of the First International Confer-
 635 ence on Human Language Technology Research*, 2001. URL <https://www.aclweb.org/anthology/H01-1069>.

636

637 Edward J Hu, Phillip Wallis, Zeyuan Allen-Zhu, Yuanzhi Li, Shean Wang, Lu Wang, Weizhu Chen,
 638 et al. LoRA: Low-rank adaptation of large language models. In *International Conference on*
 639 *Learning Representations*, 2021.

640

641 Guangming Huang, Yunfei Long, and Cunjin Luo. Similarity-dissimilarity loss for multi-label su-
 642 pervised contrastive learning. *arXiv preprint arXiv:2410.13439*, 2024.

643

644 Najoung Kim and Sebastian Schuster. Entity tracking in language models. *arXiv preprint*
 645 *arXiv:2305.02363*, 2023.

646

647 H. W. Kuhn. The hungarian method for the assignment problem. *Naval Research Logistics Quar-
 648 terly*, 2(1-2):83–97, 1955. doi: 10.1002/nav.3800020109.

649

650 Woosuk Kwon, Zhuohan Li, Siyuan Zhuang, Ying Sheng, Lianmin Zheng, Cody Hao Yu, Joseph E.
 651 Gonzalez, Hao Zhang, and Ion Stoica. Efficient memory management for large language model
 652 serving with pagedattention. In *Proceedings of the ACM SIGOPS 29th Symposium on Operating*
 653 *Systems Principles*, 2023.

648 Xin Li and Dan Roth. Learning question classifiers. In *COLING 2002: The 19th International Conference on Computational Linguistics*, 2002. URL <https://www.aclweb.org/anthology/C02-1150>.

649

650

651

652 Zheng Lian, Haoyu Chen, Lan Chen, Haiyang Sun, Licai Sun, Yong Ren, Zebang Cheng, Bin Liu, Rui Liu, Xiaojiang Peng, et al. Affectgpt: A new dataset, model, and benchmark for emotion understanding with multimodal large language models. In *Forty-second International Conference on Machine Learning*, 2025.

653

654

655

656 Dekun Lin. Probability guided loss for long-tailed multi-label image classification. In *Proceedings of the AAAI Conference on Artificial Intelligence*, volume 37, pp. 1577–1585, 2023.

657

658

659 Eneldo Loza Mencía, Moritz Kulessa, Simon Bohlender, and Johannes Fürnkranz. Tree-based dynamic classifier chains. *Machine Learning*, 112(11):4129–4165, 2023.

660

661

662 Jun-Xiang Mao, Jun-Yi Hang, and Min-Ling Zhang. Learning label-specific multiple local metrics for multi-label classification. In *Proceedings of the 33rd International Joint Conference on Artificial Intelligence*, pp. 4742–4750, 2024.

663

664

665 Junxiang Mao, Wei Wang, and Min-Ling Zhang. Label specific multi-semantics metric learning for multi-label classification: Global consideration helps. In *IJCAI*, pp. 4055–4063, 2023.

666

667

668 Brian McFee, Oriol Nieto, Morwaread M Farbood, and Juan Pablo Bello. Evaluating hierarchical structure in music annotations. *Frontiers in psychology*, 8:1337, 2017.

669

670

671 Tomas Mikolov, Kai Chen, Greg Corrado, and Jeffrey Dean. Efficient estimation of word representations in vector space. *arXiv preprint arXiv:1301.3781*, 2013.

672

673

674 Saif Mohammad, Felipe Bravo-Marquez, Mohammad Salameh, and Svetlana Kiritchenko. Semeval-2018 task 1: Affect in tweets. In *Proceedings of the 12th International Workshop on Semantic Evaluation*, pp. 1–17, 2018.

675

676

677 Eduardo Fernandes Montesuma, Fred Maurice Ngole Mboula, and Antoine Souloumiac. Recent advances in optimal transport for machine learning. *IEEE Transactions on Pattern Analysis and Machine Intelligence*, 2024.

678

679

680 Charilaos Papaioannou, Emmanouil Benetos, and Alexandros Potamianos. Lc-protonets: Multi-label few-shot learning for world music audio tagging. *IEEE Open Journal of Signal Processing*, 2025.

681

682

683 Jeffrey Pennington, Richard Socher, and Christopher D Manning. Glove: Global vectors for word representation. In *Proceedings of the 2014 Conference on Empirical Methods in Natural Language Processing (EMNLP)*, pp. 1532–1543, 2014.

684

685

686

687 Robert Plutchik. A general psychoevolutionary theory of emotion. In *Theories of emotion*, pp. 3–33. Elsevier, 1980.

688

689

690

691 Mallinali Ramírez-Corona, L Enrique Sucar, and Eduardo F Morales. Hierarchical multilabel classification based on path evaluation. *International Journal of Approximate Reasoning*, 68:179–193, 2016.

692

693

694 Paul Resnick, Yuqing Kong, Grant Schoenebeck, and Tim Weninger. Survey equivalence: A procedure for measuring classifier accuracy against human labels. *arXiv preprint arXiv:2106.01254*, 2021.

695

696

697 Ryan A Rossi, Nesreen K Ahmed, Hoda Eldardiry, and Rong Zhou. Similarity-based multi-label learning. In *2018 International Joint Conference on Neural Networks (IJCNN)*, pp. 1–8. IEEE, 2018.

698

699

700

701 James A Russell. A circumplex model of affect. *Journal of personality and social psychology*, 39(6):1161, 1980.

702 Sahand Sabour, Siyang Liu, Zheyuan Zhang, June Liu, Jinfeng Zhou, Alvionna Sunaryo, Tatia Lee,
 703 Rada Mihalcea, and Minlie Huang. Emobench: Evaluating the emotional intelligence of large lan-
 704 guage models. In *Proceedings of the 62nd Annual Meeting of the Association for Computational*
 705 *Linguistics (Volume 1: Long Papers)*, pp. 5986–6004, 2024.

706 Jordan Bennett Louis Smith, John Ashley Burgoine, Ichiro Fujinaga, David De Roure, and J Stephen
 707 Downie. Design and creation of a large-scale database of structural annotations. In *ISMIR*,
 708 volume 11, pp. 555–560. Miami, FL, 2011.

710 Aixin Sun and Ee-Peng Lim. Hierarchical text classification and evaluation. In *Proceedings 2001*
 711 *IEEE International Conference on Data Mining*, pp. 521–528, 2001. doi: 10.1109/ICDM.2001.
 712 989560.

713 Joshua B Tenenbaum, Vin de Silva, and John C Langford. A global geometric framework for
 714 nonlinear dimensionality reduction. *science*, 290(5500):2319–2323, 2000.

716 Jackson Trager, Alireza S Ziabari, Aida Mostafazadeh Davani, Prene Golazizian, Farzan Karimi-
 717 Malekabadi, Ali Omrani, Zhihe Li, Brendan Kennedy, Nils Karl Reimer, Melissa Reyes, et al.
 718 The moral foundations reddit corpus. *arXiv preprint arXiv:2208.05545*, 2022.

719 Houcemeddine Turki, Mohamed Ali Hadj Taieb, and Mohamed Ben Aouicha. Knowledge-based
 720 construction of confusion matrices for multi-label classification algorithms using semantic simi-
 721 larity measures. *arXiv preprint arXiv:2011.00109*, 2020.

723 Xiaolong Wang, Yufei Ye, and Abhinav Gupta. Zero-shot recognition via semantic embeddings
 724 and knowledge graphs. In *Proceedings of the IEEE conference on computer vision and pattern*
 725 *recognition*, pp. 6857–6866, 2018.

727 Xuewei Wang, Weiyan Shi, Richard Kim, Yoojung Oh, Sijia Yang, Jingwen Zhang, and Zhou Yu.
 728 Persuasion for good: Towards a personalized persuasive dialogue system for social good. *arXiv*
 729 *preprint arXiv:1906.06725*, 2019.

730 Zeyu Wang, Haoran Xiong, Qitong Wang, Zhenying He, Peng Wang, Themis Palpanas, and Wei
 731 Wang. Dimensionality-reduction techniques for approximate nearest neighbor search: A survey
 732 and evaluation. *IEEE Data Eng. Bull.*, 48(3):63–80, 2024. URL <http://sites.computer.org/debull/A24sept/p63.pdf>.

734 Thomas Wolf, Lysandre Debut, Victor Sanh, Julien Chaumond, Clement Delangue, Anthony Moi,
 735 Pierrick Cistac, Tim Rault, Rémi Louf, Morgan Funtowicz, Joe Davison, Sam Shleifer, Patrick
 736 von Platen, Clara Ma, Yacine Jernite, Julien Plu, Canwen Xu, Teven Le Scao, Sylvain Gugger,
 737 Mariama Drame, Quentin Lhoest, and Alexander M. Rush. Transformers: State-of-the-art natural
 738 language processing. In *Proceedings of the 2020 Conference on Empirical Methods in Natural*
 739 *Language Processing: System Demonstrations*, pp. 38–45, Online, October 2020. Association for
 740 Computational Linguistics.

743 A SINGLE-STEP MATCH

745 To illustrate the limitations of relying on only one direction of alignment (precision or recall), we
 746 present worst-case scenarios in Figure 5. Algorithms that condition on cardinality, such as Turki
 747 et al. (2020), are not immune: arbitrarily many predictions may cluster around a single gold label, or
 748 vice versa, particularly in continuous spaces. Even the examples in Figure 1 (and its flipped version)
 749 already expose the weaknesses of single-step precision or recall, without resorting to extreme cases.

750 Beyond single-step precision or recall, the Hungarian algorithm (Kuhn, 1955) is another potential
 751 approach. However, because it enforces one-to-one matching between equinumerous sets, it must
 752 discard one of two equally close but inexact predictions by assigning it to a dummy zero match.
 753 This produces unfair penalties, even when all relevant subspaces of the gold label space are covered
 754 without over-prediction (Figure 6). Similar issues when using Optimal Transport or Wasserstein
 755 distance (Montesuma et al., 2024) to measure the similarity between two sets with arbitrary sizes
 due to the constraint of deriving a single distribution from the set.

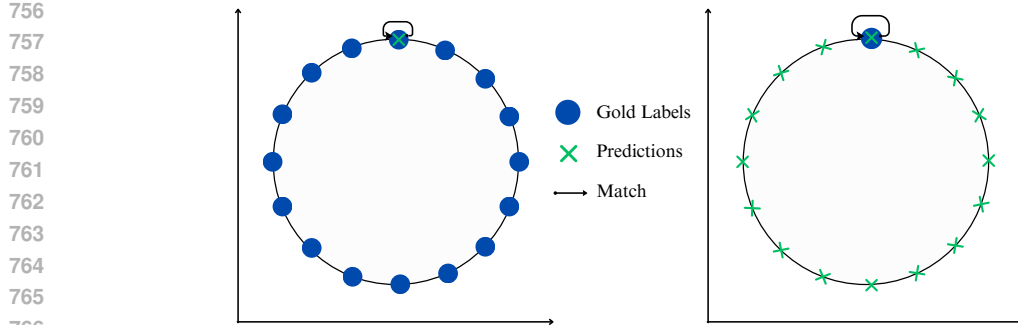


Figure 5: Worst-case scenarios for using only precision (left) and recall (right)

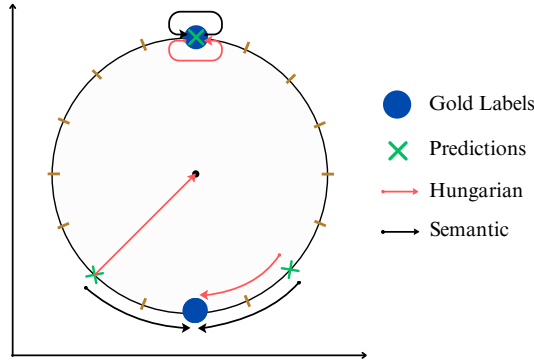


Figure 6: Comparison between our matching algorithm and the Hungarian match: The Hungarian algorithm requires equinumerous sets, thus discarding one of the two equidistant predictions of the model, an unfair penalty.

A natural extension is to patch the Hungarian algorithm by assigning unmatched labels to their closest neighbor. Yet this hybrid approach sacrifices interpretability and introduces new failure modes. Under an arithmetic mean, unmatched gold labels can be drowned out by artificially many correct matches, allowing the metric to be gamed through over-prediction (Figure 7i). Using a harmonic mean avoids this but over-penalizes a single missed label (Figure 7ii). Extending Optimal Transport to unbalanced scenarios (Montesuma et al., 2024) where sets might have different cardinalities requires balancing many hyperparameters on top of the similarity matrix.

Our Semantic F1 avoids these pitfalls. By separating over-prediction and under-coverage into two interpretable steps (semantic precision and semantic recall) and combining them with a harmonic mean, it faithfully balances errors on both sides. When the similarity matrix is the identity, this formulation collapses exactly to standard F1, preserving its robustness while extending it into the semantic domain. Unlike single-step or Hungarian-style approaches, our method does not assume equal cardinality of label sets, nor does it force spurious matches to distant labels. Every prediction and every gold label contributes to the final value, enabling a more nuanced and fine-grained evaluation.

In summary, previous similarity-based metrics suffer from unfair penalties, unintuitive averaging, or restrictive assumptions. Our two-step Semantic F1 retains the interpretability and grounding of precision and recall, extends the robustness of F1 into semantic settings, and provides a more faithful evaluation of multi-label predictions.

B HOW TO BUILD YOUR SIMILARITY MATRIX

In this section, we go into more detail about the ways we created the similarity matrix in this work.

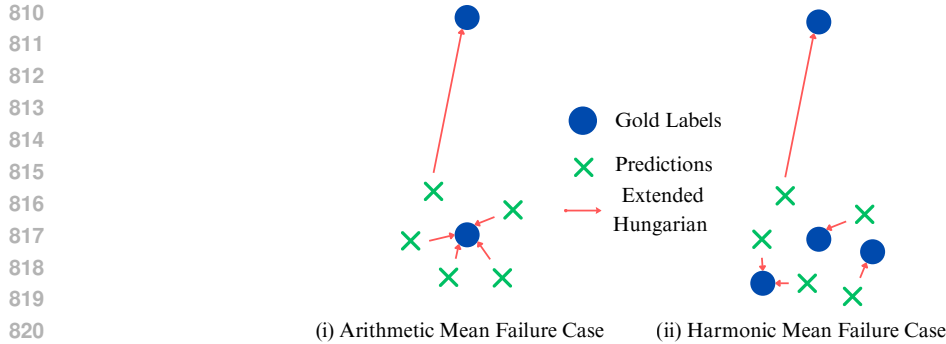


Figure 7: Example failure modes of potential extensions for the Hungarian algorithm. (i) Using the arithmetic mean drowns out under-coverage; (ii) The harmonic mean overly penalizes for a single missed gold label. Note that the clustering of the gold labels in case (ii) is done for visual purposes only, and not required for it to be a failure mode. In contrast, our two-step algorithm (i) uses recall to isolate under-coverage from the correct predictions, and (ii) averages out the missed gold label with the many covered gold labels in the recall step.

829 **Euclidean distance.** We can use $\|\cdot\|_2$ to compute the distance between embeddings in what was
830 assumed a metric space (§F.3). There, we used standard practice to convert the Euclidean distance to
831 a similarity score as $S(x, y; \|\cdot\|_2) = 1/(1 + \|x - y\|_2)$. Since $\|\cdot\|_2 \geq 0 \Rightarrow S(x, y; \|\cdot\|_2) \in [0, 1]$, with
832 $S(x, y; \|\cdot\|_2) \rightarrow 0$ when $\|x - y\|_2 \rightarrow +\infty$. Based on the baseline differences between embeddings,
833 a scaling factor may be appropriate to amplify or dampen the distance: $S(x, y; \|\cdot\|_2) = 1/(1 +$
834 $\beta\|x - y\|_2)$ in order to, in turn, amplify or dampen the difference in partial credit between labels.
835 For instance, in a space where $\min_{(a, b) \in \mathcal{L}^2} \|a - b\|_2 = 10$, β can be set to $1/10$ to make partial
836 credit stronger in the space, as for practical purposes even a minimum distance of 10 might result
837 in $S \approx I$ for all practical intents and purposes. Moreover, the embeddings can be normalized, or
838 lower and higher-order distances can be used, like $\|\cdot\|_1, \|\cdot\|_3, \dots, \|\cdot\|_\infty$, that might produce more
839 meaningful similarity values. This method allows us to use, e.g., word embeddings for the labels in
840 a setting, and construct a similarity matrix. It is also suitable for use in regression settings, as it can
841 be computed online for each example.

842 **Cosine similarity.** Cosine similarity is used similarly to measure similarity (distance) in a metric
843 embedding space. Its range of values is $[-1, 1]$, hence we simply normalize to $[0, 1]$ as $0.5 + s/2$.
844 Again, scaling can be applied to the values depending on how quickly we want the values to go to
845 0, for example by squaring or cubing the normalized values. A constant normalization factor $1/\beta$
846 results in perfectly aligned embeddings (meaning even identical embeddings) having a similarity of
847 $1/\beta$, which is usually not desirable.

848 **Correlations** The correlations should be computed outside the evaluation set to ensure the general-
849 alization of the evaluation. Similar to cosine similarity, we use an affine normalization to map the
850 values to the $[0, 1]$ range. One interesting side-effect of using correlations is that this is a purely
851 data-driven method, whereas the previous two may be applied to a theoretical space like Plutchik
852 (1980)'s wheel of emotions. Moreover, it does not assume a metric space, so it can be used to create
853 a similarity matrix in non-metric settings, as is the case for moral foundations. Normalization needs
854 to be done in a similar manner to cosine similarity.

855 **Hierarchy** While we do not perform any experiments with it, we showcase theoretically how to
856 use a label hierarchies for the Semantic F1 (Figure 8). In this case, the distance between two labels
857 is their shortest distance in the hierarchy graph, potentially weighted by edge weights. We can use
858 that similarly to the Euclidean distance to derive similarities. This approach might be useful for
859 settings with a hierarchical ontology, like music tagging (Smith et al., 2011), biological tasks, etc.

860 **Associative and Semantic Relations** A critical limitation of some of the aforementioned ap-
861 proaches lies in the distinction between associative and semantic similarity when deriving similarity
862 matrices from embeddings or correlations. Word embeddings and co-occurrence statistics capture

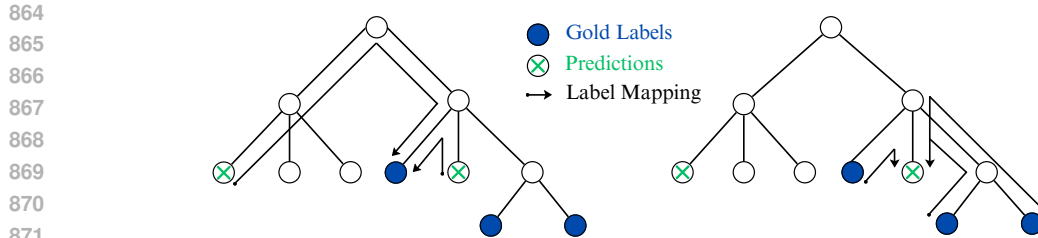


Figure 8: Example shortest paths in a label hierarchy for both steps of our algorithm.

distributional patterns, but this associative similarity may poorly represent the conceptual relatedness needed for meaningful evaluation. For instance, “doctor” and “patient” exhibit high embedding similarity due to frequent co-occurrence, yet confusing these labels in a medical classification task should not receive substantial partial credit. When we suggest using embedding distances or training correlations to construct similarity matrices, we essentially delegate core evaluation philosophy to statistical patterns rather than meaningful conceptual relationships. This approach may succeed when distributional and semantic similarity align, as is the case with ontologies fuzzy class boundaries, where co-occurrence does reflect semantic similarity, but also partially reflects the confusion of the concepts by humans due to that similarity, but fails systematically when they diverge, a common occurrence in specialized domains where technical precision matters more than linguistic association.

An interesting prospect is a per-item or per-annotator similarity matrix. Some label relationships could conceivably slightly change between examples, depending on the stimulus. For an even more accurate evaluation, the similarity could be adjusted based on gold information about the labels of the stimulus. For example, using annotator confusion for each example could inform the similarity matrix. However, using the stimulus itself to modify the similarity matrix, at least from the user perspective, would be circular: if we knew the ground-truth way to modify the similarity matrix appropriately, then we would know how to perform the classification itself. From the data distributor’s side, this is an interesting application for closed evaluations. By not sharing the modified similarity matrix, the distributor is not leaking additional information about the test labels, and can use information from the distribution of labels to modify the similarity matrix in a principled way.

C INTERPRETATION OF SIMILARITIES AND THE IDENTITY MATRIX

Care is required when interpreting similarity matrices, particularly in relation to the identity matrix.

Metric-based similarities. When similarity is derived from distances in a metric space (e.g., Euclidean), the similarity matrix approaches the identity as distances grow large ($D \rightarrow +\infty$). In practice, sufficiently separated categories behave as orthogonal, and the metric smoothly collapses to standard F1 when $S = I$.

Cosine and correlation similarities. However, in the case where values outside the range of $[0, 1]$ happen to be used, like correlations or the cosine similarity, then the interpretation of the similarity values, including the similarity of zero in the identity matrix, is trickier. That is because a normalized value of 0 for correlation corresponds to anticorrelated labels, not uncorrelated labels. Nevertheless, for practical purposes, setting S to be 0.5 outside the diagonal, the mathematically appropriate value, produces the same or similar ranking between predictions, making it effectively equivalent to $S = I$, which has the nice property of collapsing to the standard F1 score.

Design choices. We avoid allowing $S_{a,b} \in [-1, 1]$ directly, as this would require redesigning the harmonic mean to handle negative values. Instead, our normalization choices preserve the desirable property that Semantic F1 reduces exactly to standard F1 under $S = I$, while still accommodating richer similarity structures in practice.

In summary, similarity matrices can be constructed from metric distances, embeddings, correlations, or hierarchies. Each choice encodes different assumptions about the label space, but by design Semantic F1 always falls back to hard F1 when the matrix is the identity, ensuring interpretability and robustness.

D EDGE CASES AND VARIANTS

In this section, we elaborate on the formulas presented in the main text, presenting how we handle edge cases. First, for the BestMatch algorithm from Eq. 1, the complete formula is

$$\text{BestMatch}(A, B, S) = \begin{cases} \frac{1}{|A|} \sum_{a \in A} \max_{b \in B} S_{ab} & \text{if } A \neq \emptyset, B \neq \emptyset, \\ 1 & \text{if } A = \emptyset, B = \emptyset, \\ 0 & \text{otherwise.} \end{cases} \quad (14)$$

For the pointwise Semantic F1 score in Eq. 4, the full formulation is:

$$\text{SeF1}_i = \begin{cases} \frac{2 \cdot \text{Precision}_i^s \cdot \text{Recall}_i^s}{\text{Precision}_i^s + \text{Recall}_i^s} & \text{if } \text{Precision}_i^s + \text{Recall}_i^s \neq 0, \\ 0 & \text{otherwise.} \end{cases} \quad (15)$$

For the micro variant, we will first define precision and recall explicitly based on the global counts from Eq. 7, 8, 9:

$$\text{Precision}_{\text{micro}}^s = \frac{TP}{TP + FP} \quad (16)$$

$$\text{Recall}_{\text{micro}}^s = \frac{TP}{TP + FN}. \quad (17)$$

Similar to the pointwise Semantic F1 score, the edge cases of the Micro Semantic F1 score are:

$$\text{SeF1}_{\text{micro}} = \begin{cases} \frac{2 \cdot \text{Precision}_{\text{micro}}^s \cdot \text{Recall}_{\text{micro}}^s}{\text{Precision}_{\text{micro}}^s + \text{Recall}_{\text{micro}}^s} & \text{if } \text{Precision}_{\text{micro}}^s + \text{Recall}_{\text{micro}}^s \neq 0, \\ 0 & \text{otherwise.} \end{cases} \quad (18)$$

For the Semantic Macro F1 score, the per class Semantic F1 score is:

$$\text{TP}_c = \sum_{i=1}^n \begin{cases} S_{M_{P,T}(c),c} & \text{if } c \in P_i \text{ and } M_{P,T}(c) \text{ exists} \\ 0 & \text{otherwise} \end{cases} \quad (19)$$

$$\text{FP}_c = \sum_{i=1}^n \begin{cases} 1 - S_{M_{P,T}(c),c} & \text{if } c \in P_i \\ 0 & \text{otherwise} \end{cases} \quad (20)$$

$$\text{FN}_c = \sum_{i=1}^n \begin{cases} 1 - S_{c,M_{T,P}(c)} & \text{if } c \in T_i \\ 0 & \text{otherwise} \end{cases} \quad (21)$$

D.1 WEIGHTED SEMANTIC F1

We can extend Macro Semantic F1 score to use class support (frequency in ground truth) as weights:

$$\text{SeF1}_{\text{weighted}} = \frac{\sum_{c \in \mathcal{L}} w_c \cdot \text{SeF1}_c}{\sum_{c \in \mathcal{L}} w_c} \quad (22)$$

where $w_c = \sum_{i=1}^n \mathbf{1}[c \in T_i]$.

972 E EXTRA IMPLEMENTATION DETAILS
973974 We use one Nvidia A100 to perform local inference with LLMs, and one NVIDIA RTX 6000 for
975 training of Demux and Llama. Synthetic experiments were performed on the CPU. We train Demux
976 exactly as described in the original paper Chochlakis et al. (2023a). We finetune Llama-3 1B with a
977 new classification head with QLoRA (Hu et al., 2021) of rank 4 on KVQ. During different runs of
978 LLM inference, we completely resample prompt examples.979 We use exactly the same prompt format across all 6 LLMs across all tasks besides P4G, appropriately
980 changing the instructions. An example on GoEmotions is:
981982 Classify the following inputs into none, one, or multiple the following emotions
983 per input: joy, optimism, admiration, surprise, fear, sadness and anger. Output
984 exactly these emotions and no others.985 Input: "Can I speak to the Suns' manager?"
986 {"label": ["surprise"]}988 For P4G, the corresponding presentation of the conversations in the prompts take the following
989 format:
990

991 A multi-turn conversation will be presented to you in the following format:

992 CONVERSATION:

993 "
994 conversation goes here
995 "
996 "
997998 Evaluate the last turn only for the expressed emotion of the speaker. This
999 is important; do not take into account the emotions expressed previously in your
1000 assessment, but only to contextualize the last turn. Choose none, one, or multiple
1001 of the following emotions: anger, anticipation, disgust, fear, joy, love, optimism,
1002 pessimism, sadness, surprise, trust. Pick from these emotions only. Pick emotions
1003 that are plausible under some interpretation of the stimulus, but the emotions
1004 should make sense together as a group.

1005 The response should strictly follow this format:

1006 EMOTIONS: list of emotions

1008 for example 'EMOTIONS: anger, sadness', or 'EMOTIONS: optimism, love, joy'.

1010 CONVERSATION:

1011 "
1012 Turn 0: Good Evening
1013 Turn 1: Hello there. how are you?
1014 Turn 2: I am doing well! How are doing today?
1015 Turn 3: I am doing pretty well. thanks for asking!
1016 Turn 4: I'd like to tell you about a great program I am working on! Have you
1017 ever heard of Save the Children?
1018 Turn 5: I may have in passing, but could you tell me more information about it?
1019 "
1020

1021 EMOTIONS: anticipation.

1023 F ADDITIONAL RESULTS
1024

1025 Here, we present complete results that have been delegated to the appendix due to space constraints.

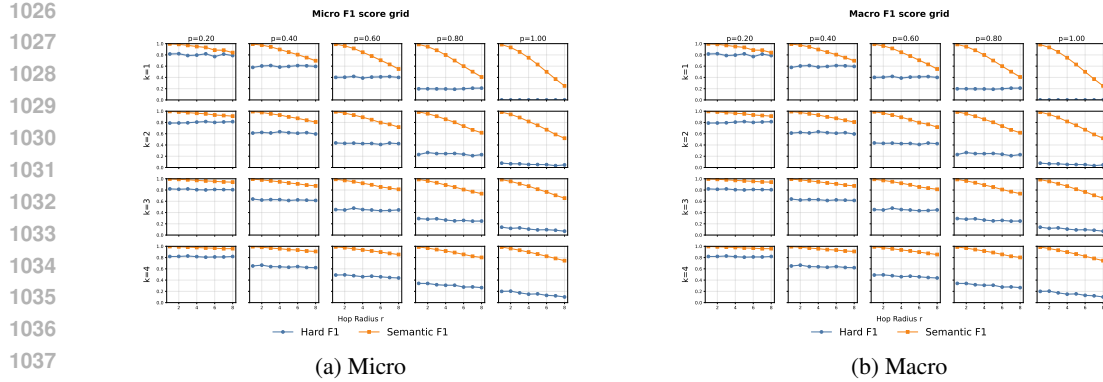


Figure 9: Hard vs Semantic F1 score across number of labels k , perturbation probability p , and hop radii r .

F.1 SYNTHETIC STUDY A

We first present how micro and macro F1 scores, hard and semantic, vary with number of labels k , perturbation probability p , and hop radius r in Figure 9. Conclusions reflect those in the main text. We also present the distribution of differences for macro and samples F1 scores in Figure 10, with similar trends shown as in the main text.

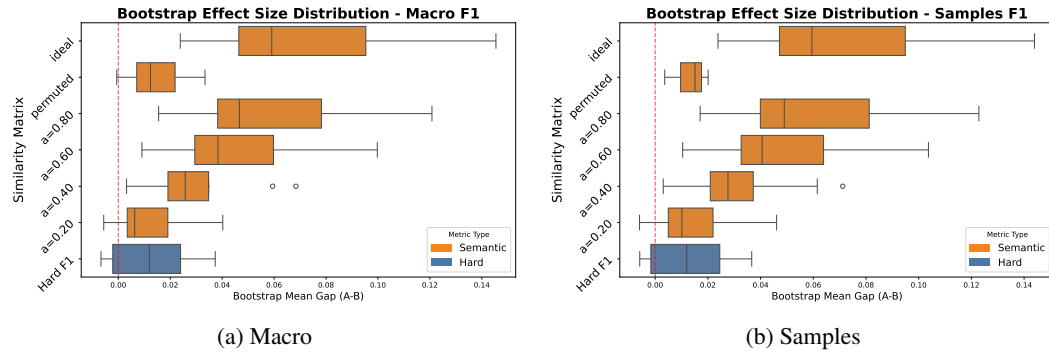


Figure 10: Distribution of differences in F1 between Near and Far predictions, aggregated across perturbation probabilities, number of labels, and radii.

We also report Kendall’s τ in Figure 11, where we quantify the degree of monotonicity in the metrics. Because we expect decreasing trends, we show negative Kendall’s τ , meaning that higher values show a higher monotonic (decreasing) trend. We see that hard metrics do not reliably have a decreasing trend, with many instances showing an increasing trend with semantically less related predictions, or a constant trend.

Finally, we also report the correlation between the rankings of the various classifiers (defined by hop radius r) across all the similarity matrix noise levels (defined by α). We aggregate results across all $p > 0$ and k . Results are shown in Figure 12. This further verifies that down to $\alpha = 0.4$, noise is still not sufficient to really obscure the information we can derive for our classifiers from Semantic F1.

F.2 SYNTHETIC STUDY B: BIMODAL HEURISTIC VS. FINE-GRAINED PREDICTOR

Motivation We test whether Semantic F1 properly penalizes “coarse correctness” when a predictor captures the correct *mode* but misses fine-grained labels. For example, some predictors might solely rely on the sentiment of a stimulus rather than finding the specific emotion, predicting the same positive or negative emotions depending on the identified sentiment. Intuitively, we would want a more fine-grained classifier, which might still make small errors, to be preferred by our met-

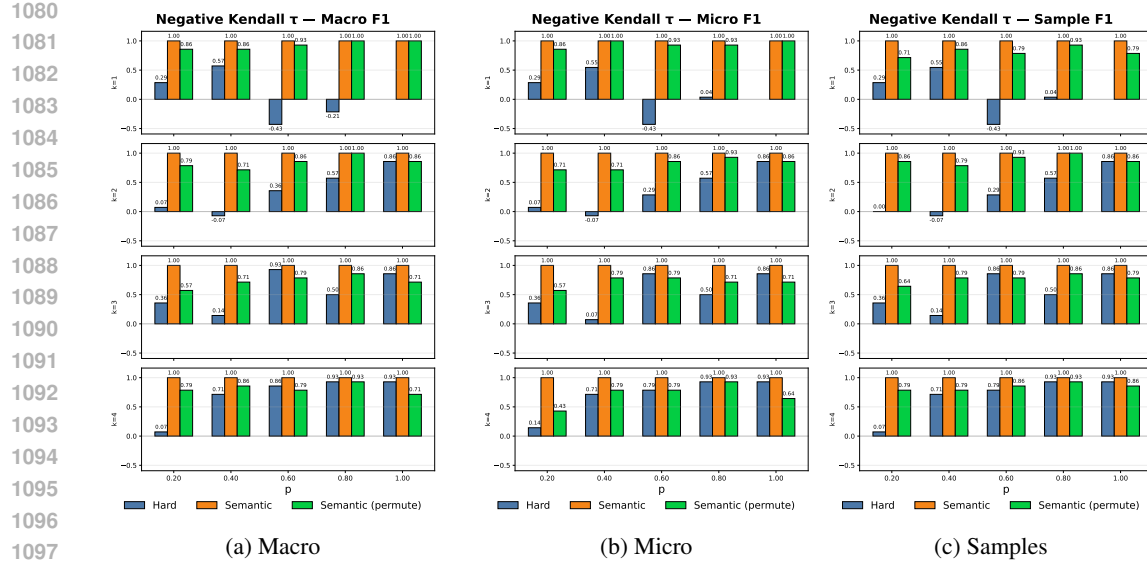


Figure 11: Negative Kendall's τ (higher is better) across settings.

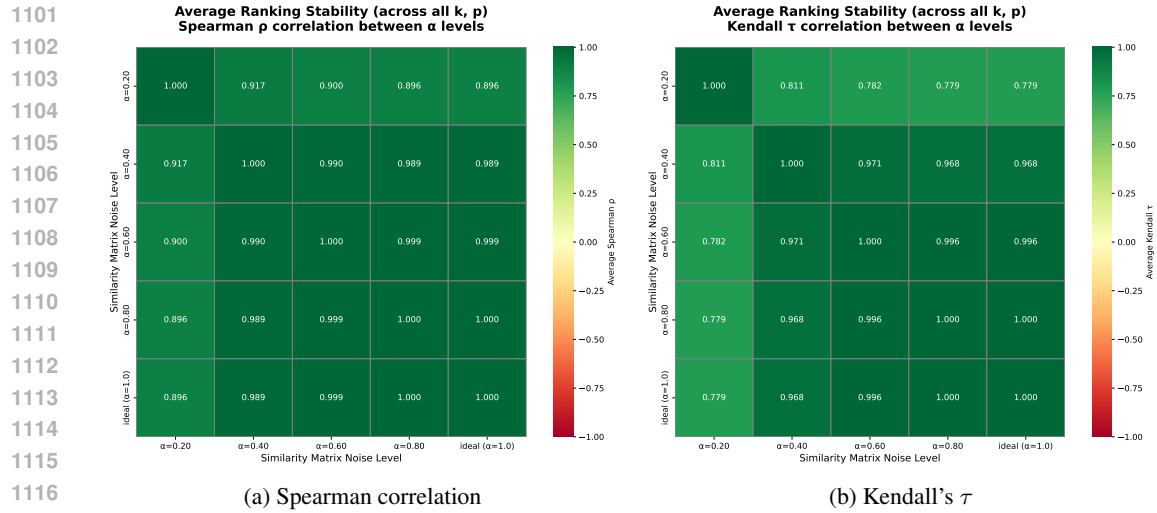


Figure 12: Micro F1 ranking stability: Spearman correlation and Kendall’s τ , aggregated across p and k , of the ranking of classifiers defined by their hop radius r .

rics. We construct a bimodal synthetic setting atop a circular label geometry (again, see the individual components in Figure 14) and compare Hard vs. Semantic F1 under controlled mode-selection behavior.

Setup. To extend the setup, we define two latent modes on the circle (positive and negative) using von Mises-like weights with concentration κ : $w_{\text{pos}}(j) \propto e^{\kappa \cos \theta_j}$ and $w_{\text{neg}}(j) \propto e^{\kappa \cos(\theta_j - \pi)}$. To generate gold sets, we first choose a mode with imbalance ratio $\rho \in \{0.25, 0.5, 0.75\}$, then sample $k \in \{2, 3\}$ labels from that mode's distribution. We evaluate prototype-based predictors that operate at the mode level: (i) **Prototype-Bimodal**: Determine the gold's dominant mode by summing mode weights over gold labels; predict that mode's $m \in \{2, 3, 4\}$ prototype labels with probability $q \in \{0, 0.2, 0.4, 0.6, 0.8, 1\}$, otherwise predict the opposite mode's prototypes. (ii) **Prototype-Within-Mode**: Choose the gold's mode with probability q then sample k labels from a distribution peaked on that mode's prototypes (tail controlled by β), otherwise from the opposite

mode. (iii) **Baselines:** Perturbation predictors from Study A.1 for reference, with $p = 1.0$ (exact matches only by chance). We use $n=24$ labels and 1000 examples per configuration.

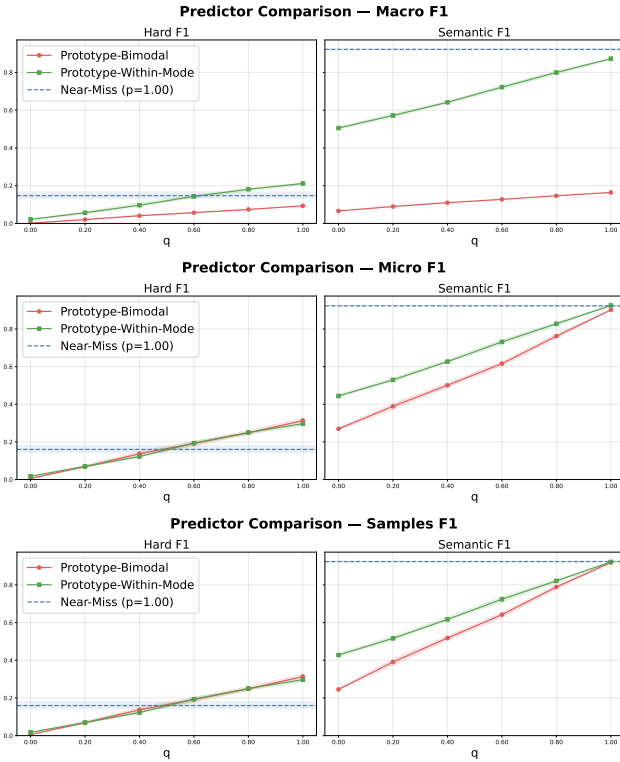


Figure 13: Comparison of bimodal heuristic classifiers compared to near-miss ‘intelligent’ classifier.

Metrics and statistics. We report Hard F1 (micro/macro/samples) and Semantic F1 (micro/macro/samples). For probability sweeps, we plot metric vs. q with $B = 20$ bootstrap 95% CIs for the prototype predictors and overlay a horizontal reference for a perturbation baseline.

Results. We compare the performance of the heuristic classifiers across different correct mode probability q with the performance of the near miss, intelligent classifier in Figure 13. We see that across all different metrics, the heuristic classifiers outperform or are comparable to the intelligent classifier in hard scores, but that is not necessarily the case with the semantic scores. This is especially the case with samples F1. We conclude, therefore, that hard metrics cannot distinguish between mode heuristics effectively, whereas semantic metrics have the ability to.

F.3 SYNTHETIC STUDY C: NON-METRIC SPACES

Motivation We stress-test Semantic F1 on a union-of-manifolds label space to assess whether geometry-aware similarities continue to distinguish near vs. far perturbations when labels lie on mixed structures. By contrasting ideal similarities with misaligned proxies (namely, a misguided assumption of a metric space), we show how naive metric choices can collapse Semantic F1 back toward hard F1 behavior, providing valuable guidance for practitioners. While the specific geometry is indeed synthetic (no immediate real world parallel)

Setup. Using the ring structure from Study A, we create a disjoint manifold as the union of ring structures, shown in Figure 14. Within each ring structure, the space is metric, but the disjoint manifold structure dictates that this is not so across manifolds. We modify the near-miss and far-miss predictors to include an additional parameter, p_{jump} . This quantifies the probability that a prediction will hop between manifolds. This is on top of p , which dictates the probability of a hop from gold labels to predictions. For simplicity and without loss of generality, we assume symmetric structures

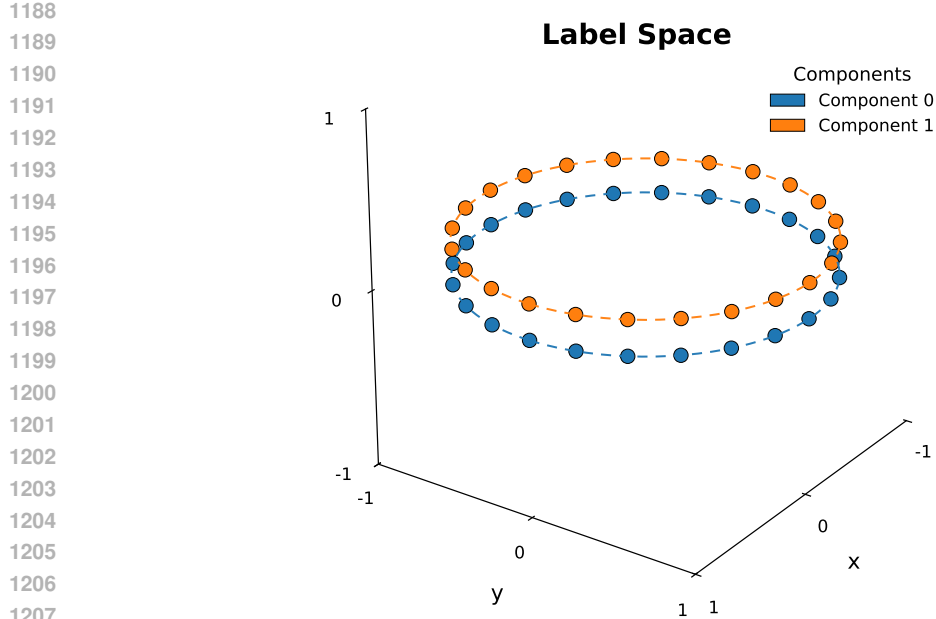


Figure 14: Non-metric label space: Disjoint union of manifolds

between rings, creating pairs of labels from each manifold. Similarity from a label of the other manifold is maximum at its pair label, and decays identically to the within-manifold behavior. Each configuration evaluates Semantic F1 under three matrices: (i) **Ideal**: geometry-derived similarities that respect manifold connectivity. (ii) **Permuted**: row-permuted control mirroring Study A.1 to break structure. (iii) **Deceptive Euclidean**: $1/(1 + \|\cdot\|_2)$ over points in three-dimensional space, assuming unit radius and a distance of 0.2 between rings, causing parallel manifolds to appear adjacent.

Metrics and statistics. We report hard F1 alongside Semantic F1 for each similarity matrix. We sweep $k \in \{1, 2, 3, 4\}$, $p = 1$, near radii $\{1, 2, 3, 4\}$, far radii $\{4, 5, 6, 7\}$, and $p_{jump} \in \{0, 0.2, 0.4, 0.6, 0.8, 1\}$. We present a grid of k - p_{jump} plots with varying radii. We set $n = 48$ with each ring having 24 labels, making each identical to synthetic study A.

Results. In Figure 15, we see that the permuted and the deceptive similarity matrices, as well as the hard F1 score are invariant to the increase of p_{jump} . In addition, the permuted similarity matrix and hard F1 score are invariant to the increase of the hop radius, as we saw in study A as well (§4.3.1). In contrast, we see that Semantic F1 decreases linearly with hop radius when the hops happen in the same manifold, whereas it is relatively insensitive to the hop radius when most errors land in a different manifold (as all the labels are considered very distant in semantic space). It also decreases linearly with p_{jump} , as desired. Moreover, from Figure 16, we see that the moderately misspecified similarity matrix with $\alpha = 0.5$ also shows the same separability with the ideal matrix. Additionally, we see that the deceptive matrix shows much higher separability between predictors, when that should not be the case given the similarly low scores of cross-manifold jumps. Hard F1 and permuted similarity matrix show the same behavior, clustered around 0.

F.4 SYNTHETIC STUDY D: EMPIRICAL COMPARISON TO BASELINES

Motivation. We compare Semantic F1 to previous similarity-based single-step metrics, in particular with semantic recall, semantic precision motivated by the work of Turki et al. (2020), and the extended Hungarian, which we develop as a strong baseline and present in §A. We show how their failure cases can manifest in plausible settings and affect their ability to capture nuances in predictive behavior, in contrast to the Semantic F1 score.

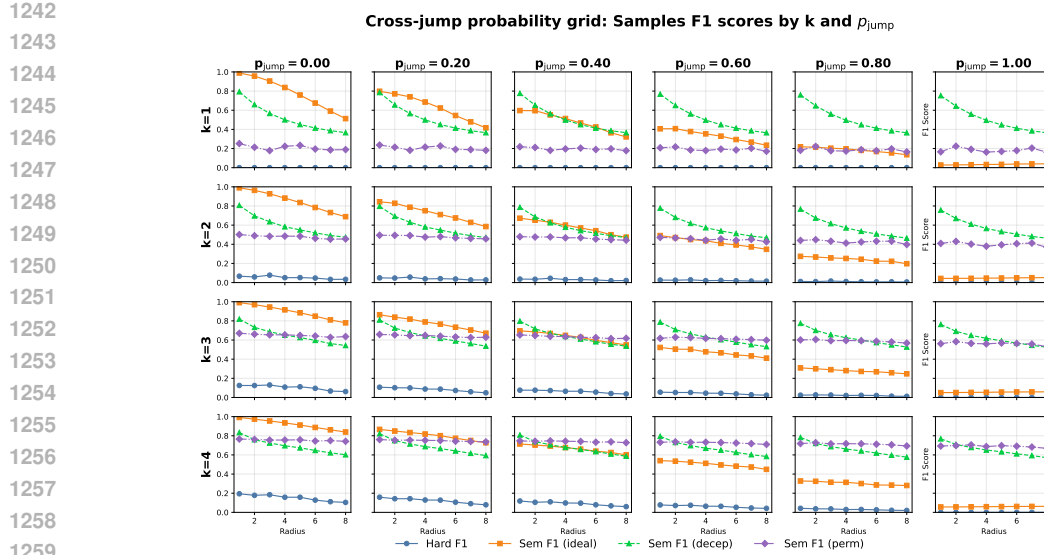


Figure 15: Hard vs semantic samples F1 score across number of labels k , cross-manifold hop probability p_{jump} , and hop radii r . Semantic F1 is also shown with a deceptive Euclidean-based similarity matrix, and a permuted similarity matrix.

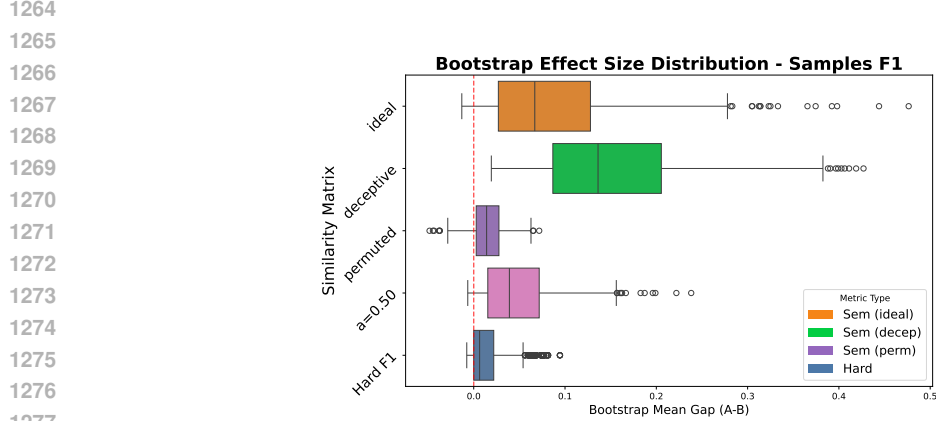
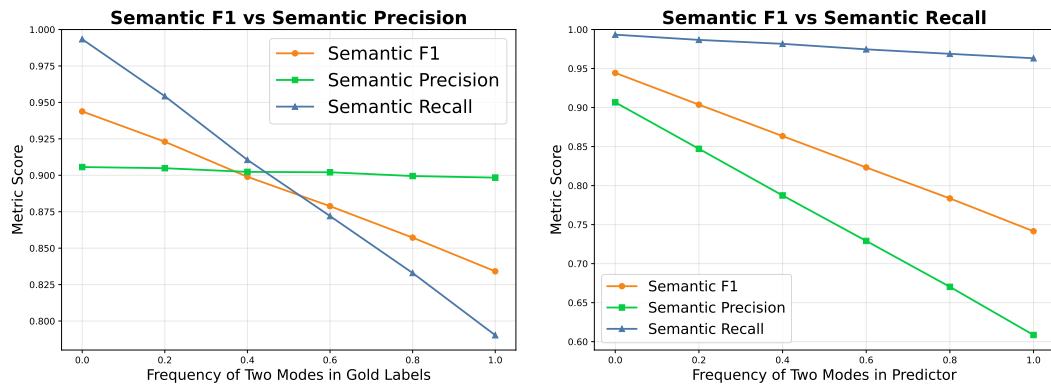


Figure 16: Distribution of differences in F1 between Near and Far predictions, aggregated across across-manifold jump probabilities, number of labels, and radii.

Setup. Using the ring geometry from synthetic study A, gold and predicted label sets are sampled around mode centers via softmax-weighted cosine similarity. We vary the number of gold labels k , a hop/perturbation probability p , the frequency that gold or predicted labels are bimodal p_b , and, in one scenario, the number of predicted labels. Three stress tests are run: (i) *Precision stress test (bimodal gold, unimodal predictor)*. A proportion p_b of examples have bimodal gold labels (two opposite ring modes). The predictor remains unimodal and, on bimodal examples, only hops around one mode in label space with probability p . We compare Semantic F1 to semantic precision as the frequency of bimodality varies, and show recall for reference. (ii) *Recall stress test (unimodal gold, bimodal predictor)*. Gold is always unimodal. The predictor is bimodal with controlled frequency and, when bimodal, predicts $k/2$ labels from the gold mode and $k/2$ from another mode; otherwise it locally hops around the gold mode. We compare Semantic F1 to semantic recall across the predictor’s bimodality frequency, and show precision for reference. (iii) *Hungarian stress test (bimodal gold, unimodal predictor, varying prediction counts)*. Gold may be uni- or bimodal as above. The predictor outputs a controlled number of labels centered on one mode, sweeping the number of predictions while holding k fixed. We compare Semantic F1 to the extended Hungarian score. All

1296 comparisons use sample Semantic F1 as the most natural comparison to the sample-based Hungarian
 1297 score.
 1298

1299 **Metrics and statistics.** For each configuration (values of k , bimodality frequency, p , and, when
 1300 applicable, number of predictions), we generate synthetic datasets of 1000 examples per configura-
 1301 tion and report means. Plots aggregate over nuisance variables (e.g., averaging across k and p
 1302 where appropriate) to show mean curves for Semantic F1 and the relevant baseline. We choose
 1303 $n \in \{96, 192\}$ (to allow us to scale the number of predictions within a single space to 17 without
 1304 expanding to other subspaces in label space, and therefore get smoother curves), $k = 2$, and predic-
 1305 tive temperature of 0.1 for the Hungarian comparison, and $n = 96$, $k \in \{6, 8, 10\}$, $p = 1$, a hop
 1306 radius of 2, and gold sampling temperature of 0.05.
 1307



1320 Figure 17: Failure modes when using only semantic precision (left) and only semantic recall (right).
 1321
 1322

1323 **Results.** Figure 17 show that, as expected, *precision* fails to take into account the under-coverage
 1324 of the label space when that becomes bimodal, whereas *recall* does not penalize over-prediction
 1325 when the predictor becomes more and more bimodal in a unimodal label space. Semantic F1 prop-
 1326 erly scales down in both cases. It is worth noting that flipping gold and predicted labels in each
 1327 setting flips the metric that has a failure mode, yet Semantic F1 remains the same. In Figure 18
 1328 (figures are identical for $n = 96$ and 192, so we show only the latter.), we see how the Hungarian
 1329 algorithm rewards bad predictors. As we increase the rate of bimodal label spaces, we see that
 1330 the performance of a unimodal predictor does not decrease, as measured by the Hungarian score.
 1331 This happens because the predictor can predict the neighbors in its captured mode to artificially in-
 1332 crease its score with the Hungarian algorithm, as can be seen by the large increases in performance
 1333 when the predictor adds more and more predictions in the same region. In contrast, the Semantic
 1334 F1 seems much more moderate scaling when predictors increase within each setting, and, notably,
 1335 performance degrades as the label space becomes more bimodal. This scaling behavior in Semantic
 1336 F1, as opposed to the Hungarian algorithm, is a byproduct of the similarity matrix used and not the
 1337 method itself. For instance, if we saturate the similarity to 0 faster as we move away from each
 1338 label, for example by squaring or cubing it, the effect is eliminated for Semantic F1, but not for the
 1339 Hungarian score, as can be seen in Figure 19.
 1340

F.5 REAL STUDY A

1341 Here, we present how the results for Llama-3 1B, as shown in the main text for Demux, in Figure 20,
 1342 and how performance varies per threshold on the rest of the datasets, GoEmotion and MFRC, in
 1343 Figures 21 and 22 respectively.
 1344

F.6 REAL STUDY B

1345 For completeness, we present the full correlations for all metrics for both datasets in Figures 23, 24
 1346 and 25. As noted before, the correlations to Semantic F1 metrics are at least as large as with the
 1347 hard F1 scores in all settings, a good indicator that semantic metrics are more ecologically valid in
 1348 problems with interrelated, fuzzy labels. In Tables 2 and 3, we see that this is not in general the case
 1349

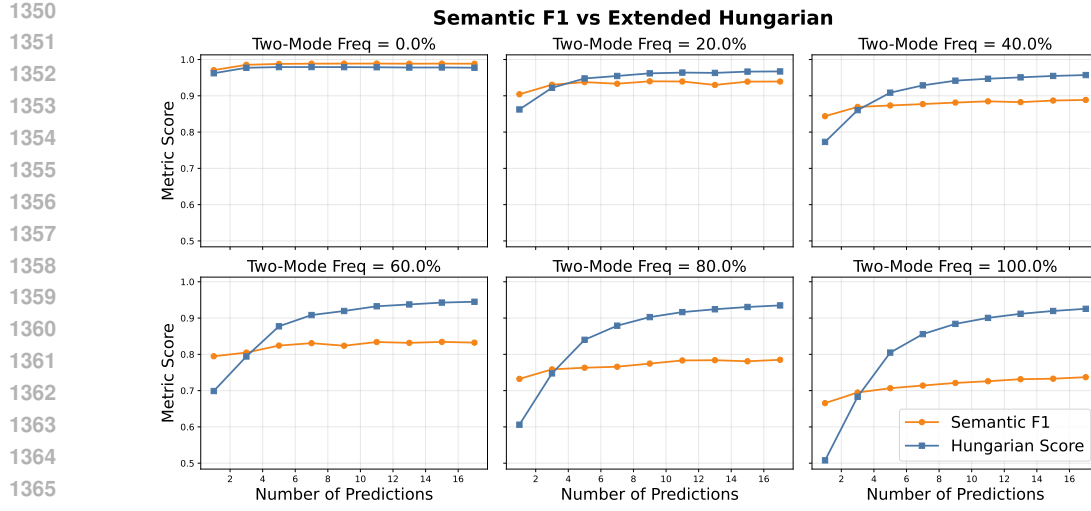


Figure 18: Semantic F1 vs Hungarian: Hungarian drowns out missed label space by predicting more and more labels around another label mode.

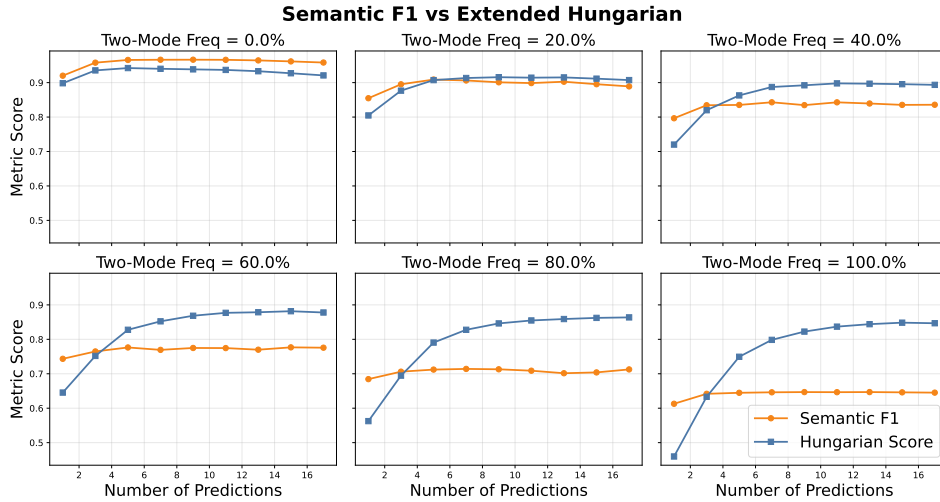


Figure 19: Semantic F1 vs Hungarian with *cubed* similarity matrix: Hungarian still scales with more predictions around one label mode.

for individual semantic components, and that in a general setting, both of them need to be combined to the Semantic F1 to provide reliable results. It is interesting to see that correlation with Semantic Precision is low; it indicates that under-coverage is an important property for emotional downstream tasks.

	Precision	Recall	Hard F1
Samples	0.348	0.754	
Micro	0.232	0.899	0.696
Macro	0.522	0.986	

Table 2: Correlations of P4G and SemEval

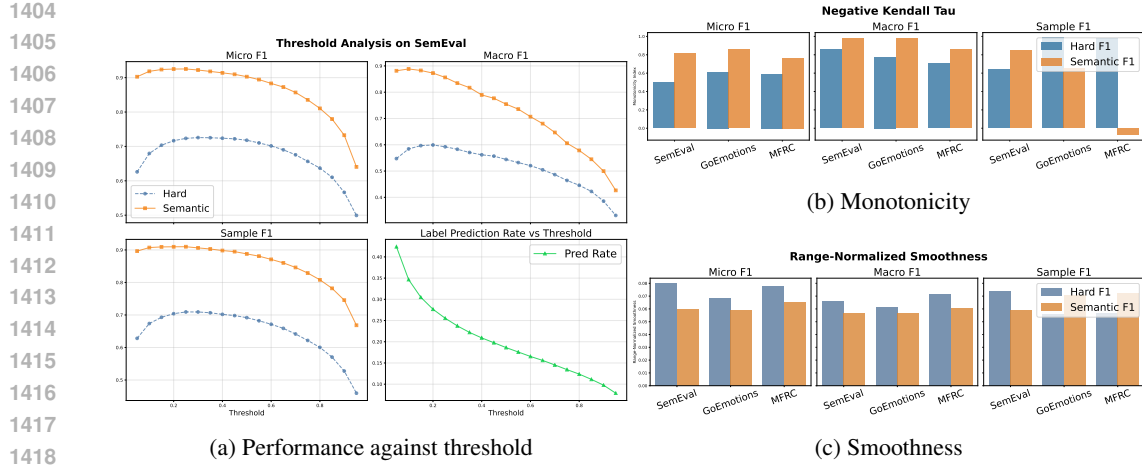


Figure 20: Threshold analysis on Llama-3 1B

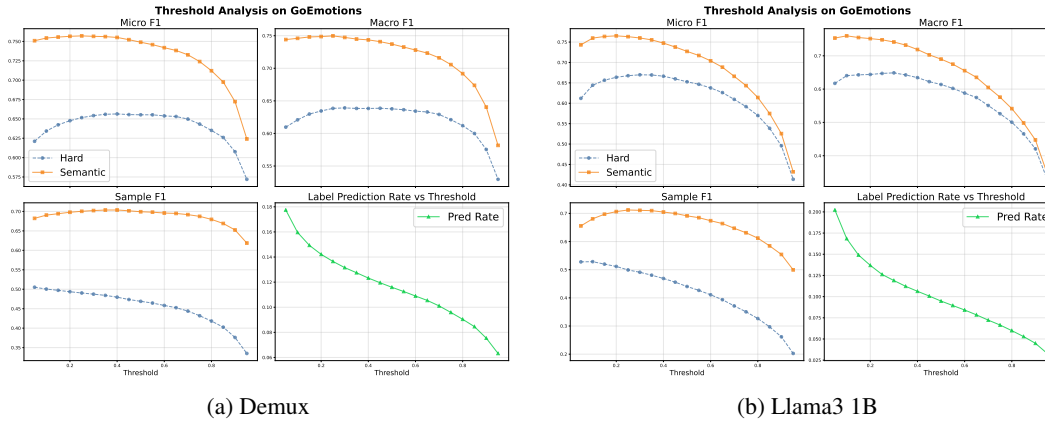


Figure 21: Semantic and hard F1 scores across probability thresholds on GoEmotions.

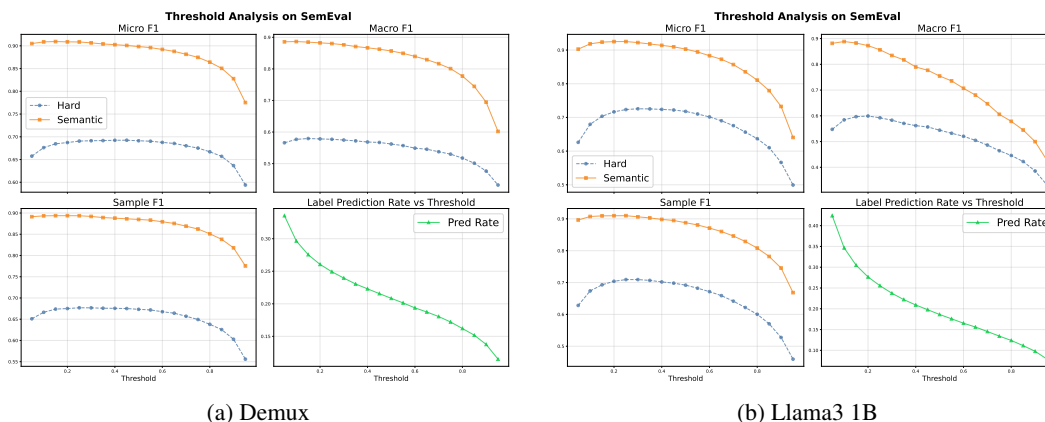


Figure 22: Semantic and hard F1 scores across probability thresholds on MFRC.

F.7 REAL STUDY C

We present detailed results on early stopping for all subjective multi-label datasets, in Figures 26, 27 and 28. Aggregated results for these datasets were already shown in Table 1. As noted, we see that semantic early stopping leads to significant gains even in hard metrics, like Jaccard Score in MFRC.

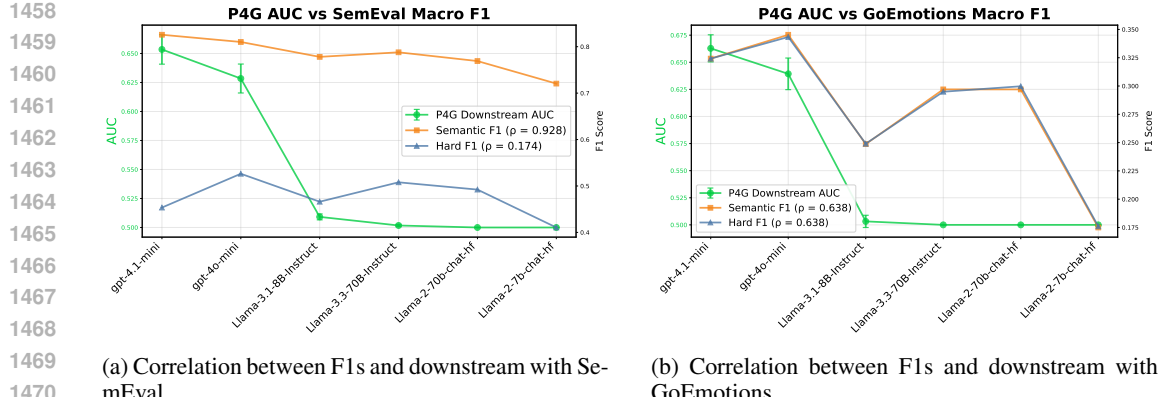


Figure 23: Ecological validity study results comparing macro Semantic F1 vs hard F1 correlation with downstream task performance across different emotion datasets

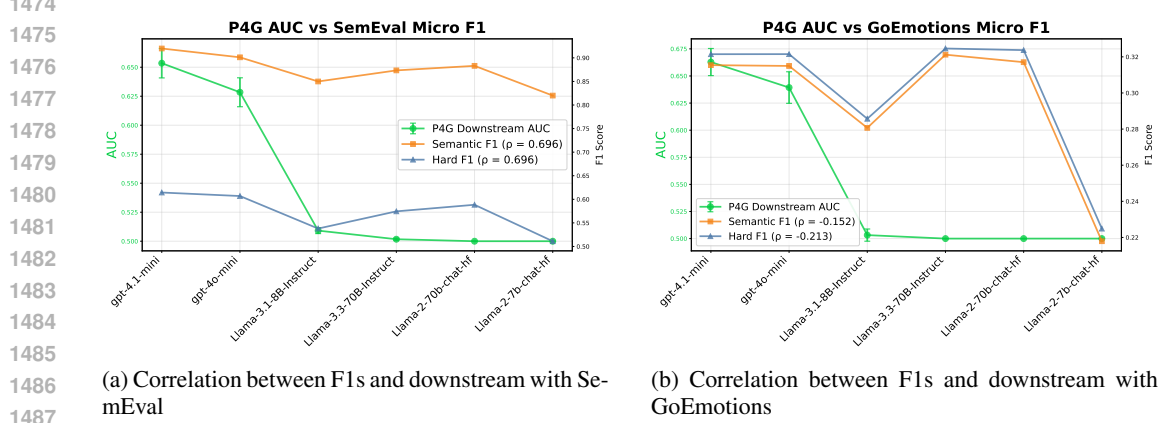


Figure 24: Ecological validity study results comparing micro Semantic F1 vs hard F1 correlation with downstream task performance across different emotion datasets

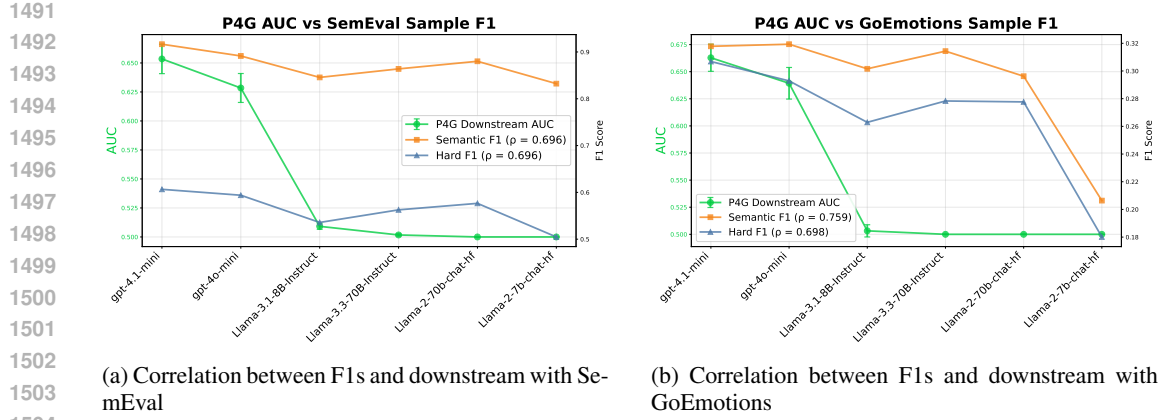


Figure 25: Ecological validity study results comparing samples Semantic F1 vs hard F1 correlation with downstream task performance across different emotion datasets

F.8 REAL STUDY D: CONVERGENT VALIDITY

We use the following additional, objective datasets to evaluate how scaling correlates between objective and subjective tasks:

		Precision	Recall	Hard F1
1512	Samples	0.334	0.880	
1513	Micro	0.575	0.941	0.698
1514	Macro	0.152	0.880	
1515				
1516				

Table 3: Correlations of P4G and GoEmotions

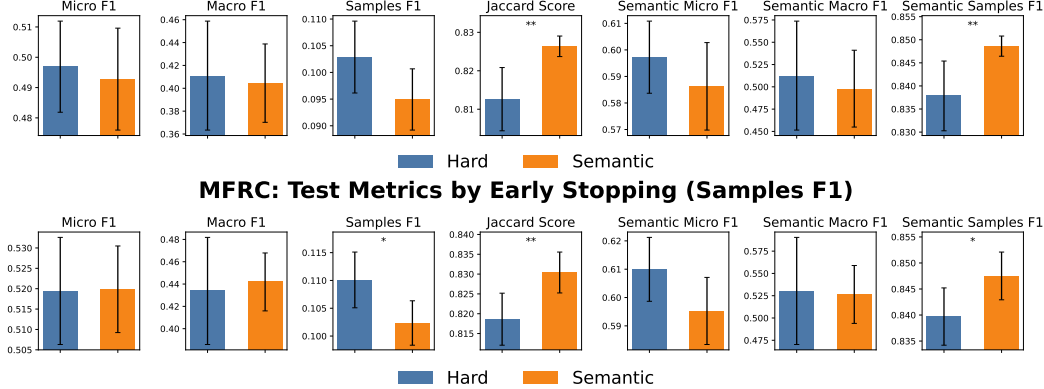
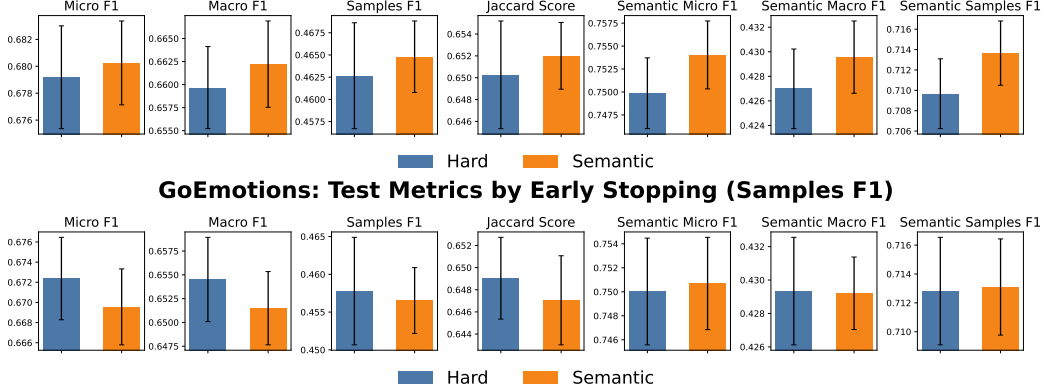
MFRC: Dev Metrics by Early Stopping (Samples F1)Figure 26: Performance comparison on MFRC across 6 F1 metrics and Jaccard Score when using hard or semantic samples F1 score as early stopping criterion. *: $p < 0.05$, **: $p < 0.01$.**GoEmotions: Dev Metrics by Early Stopping (Samples F1)**

Figure 27: Performance comparison on GoEmotions across 6 F1 metrics and Jaccard Score when using hard or semantic samples F1 score as early stopping criterion.

MovieLens (Harper & Konstan, 2015) Objective multi-label movie genre prediction based on IMDB movie summaries.

Boxes (Kim & Schuster, 2023) Objective multi-label entity tracking based on natural language description of “box” contents and “move” operations. Each box can contain none, one, or multiple objects. The dataset contains thousands of synthetic examples.

TREC (Hovy et al., 2001; Li & Roth, 2002) Objective single-label question classification benchmark, which contains annotations for the type of information the question pertains to.

Setup. We evaluate Semantic F1 on real datasets to test convergent validity: if Semantic F1 score is a better metric, then on subjective, fuzzy multi-label tasks it should align better with model capability in objective single-label and multi-label datasets compared to Hard F1 score.

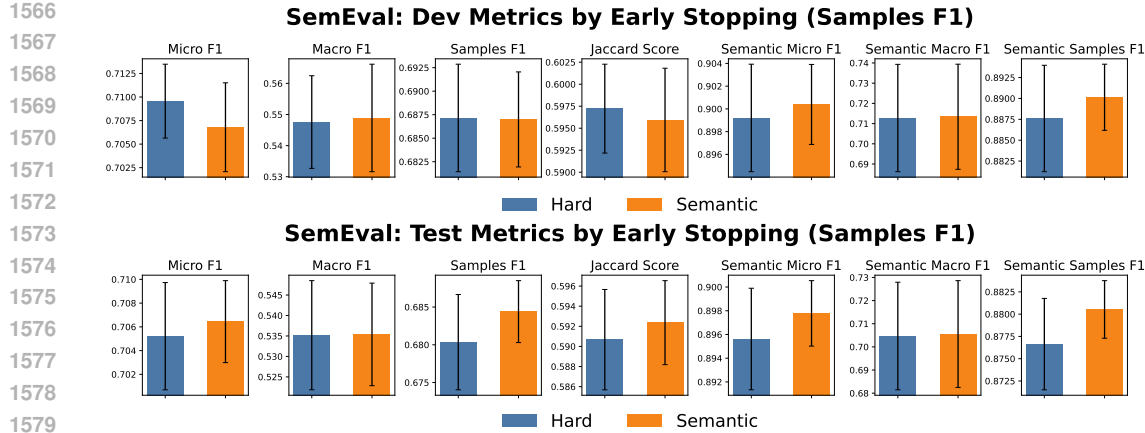


Figure 28: Performance comparison on SemEval across 6 F1 metrics and Jaccard Score when using hard or semantic sample F1 score as early stopping criterion.

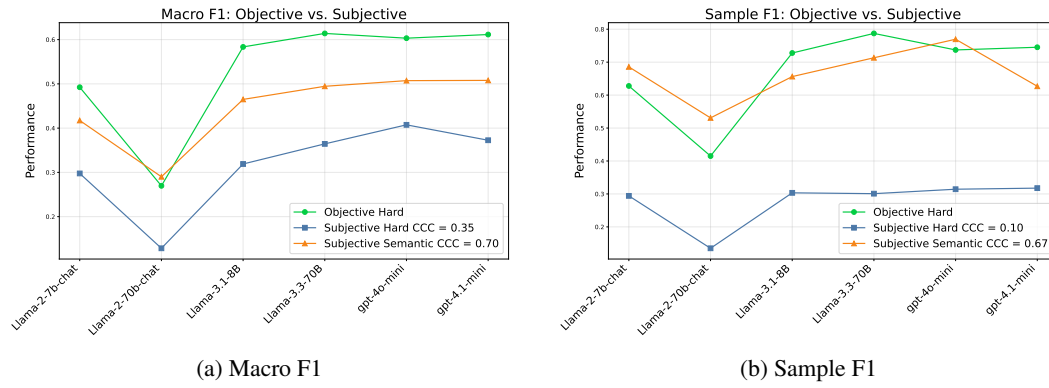


Figure 29: Semantic and hard F1 scores on subjective tasks correlated using CCC with hard F1 score performance in objective tasks.

Metrics and statistics. We compare the average performance on single-label and multi-label objective tasks, using hard F1 metrics, with the average performance on multi-label subjective tasks using semantic and hard F1 metrics (micro/macro/samples). We do not present micro F1, as it is not defined for single-label settings. We report the Concordance Correlation Coefficient (CCC) and the Spearman correlation of the metrics on the subjective tasks with the objective tasks. The CCC is employed in this scenario because performance is on the same scale for all corresponding metrics, and therefore tracking entails the element of matching the magnitude. Also, it was used as a complement to Spearman correlation, since we note that 95% CIs are large enough to make correlations and ranking volatile.

Results. Figure 29 shows the performance on objective and subjective tasks of 6 LLMs, and the CCC of the semantic and the hard subjective performance to the objective performance. We see that CCC is much higher using the Semantic F1 scores, suggesting that Semantic F1 tracks hard F1 score on objective tasks better than hard F1 on subjective tasks does. We note that Spearman correlation results are mixed; semantic macro F1 has $\rho = 0.83$, beating the $\rho = 0.77$ of hard macro F1, but hard sample F1 score beats semantic sample F1 with a Spearman correlation of $\rho = 0.66$ compared to $\rho = 0.49$. For macro F1, we also present all the objective-subjective dataset pairs in Figure 30.

G PSEUDOCODE

In this section, we present the pseudocode for BestMatch, Samples, Micro, and Macro Semantic F1 scores in Algorithms 1, 2, 3 and 4 respectively.

1620

Algorithm 1 BestMatch

1621

Require: Label set A , Label set B , Similarity matrix S

1622

similarityScores $\leftarrow \emptyset$

1623

 $M_{A,B} \leftarrow \{\}$

// label pairs hashmap

1624

for each $a \in A$ **do**

1625

 $b \leftarrow \arg \max_{x \in B} S_{a,x}$

1626

 $M_{A,B}[a] \leftarrow b$

1627

similarityScores.append($S_{a,b}$)

1628

end for

1629

 $\bar{s} \leftarrow \frac{1}{|A|} \sum_{s \in \text{similarityScores}} s$

// arithmetic mean of similarities

1630

return \bar{s}

1631

Algorithm 2 Samples Semantic F1 Score

1632

Require: Predicted sets $\{P_1, P_2, \dots, P_n\}$, True sets $\{T_1, T_2, \dots, T_n\}$, Similarity matrix S

1633

 $F1 \leftarrow 0$

// accumulator for F1 scores

1634

for $i = 1$ to n **do**

1635

prec \leftarrow BestMatch(P_i, T_i, S)

// Compute semantic precision

1636

rec \leftarrow BestMatch(T_i, P_i, S)

// Compute semantic recall

1637

 $F1 \leftarrow F1 + \frac{2 \cdot \text{prec} \cdot \text{rec}}{\text{prec} + \text{rec}} \cdot \frac{1}{n}$

// Compute harmonic mean for F1

1638

end for

1639

return $F1$

// arithmetic mean of F1 scores

1640

Algorithm 3 Micro Semantic F1 Score

1641

Require: Predicted sets $\{P_1, P_2, \dots, P_n\}$, True sets $\{T_1, T_2, \dots, T_n\}$, Similarity matrix S

1642

Initialize $TP \leftarrow 0$, $FP \leftarrow 0$, $FN \leftarrow 0$

// global semantic counts

1643

for $i = 1$ to n **do**

1644

Compute forward pairs: $F_i \leftarrow \{(p, \arg \max_{t \in T_i} S_{tp}) : p \in P_i\}$

1645

Compute reverse pairs: $R_i \leftarrow \{(t, \arg \max_{p \in P_i} S_{tp}) : t \in T_i\}$

// Accumulate semantic true positives

1646

for each $p \in P_i$ **do**

1647

if p has forward match $t^* \in T_i$ **then**

1648

 $TP \leftarrow TP + S_{t^*p}$

1649

end if

1650

end for

1651

// Accumulate semantic false positives

1652

for each $p \in P_i$ **do**

1653

if p has forward match $t^* \in T_i$ **then**

1654

 $FP \leftarrow FP + (1 - S_{t^*p})$

1655

else

1656

 $FP \leftarrow FP + 1$

1657

end if

1658

end for

1659

end for

1660

// Accumulate semantic false negatives

1661

for each $t \in T_i$ **do**

1662

if t has reverse match $p^* \in P_i$ **then**

1663

 $FN \leftarrow FN + (1 - S_{tp^*})$

1664

else

1665

 $FN \leftarrow FN + 1$

1666

end if

1667

end for

1668

end for

1669

// Compute global precision and recall

1670

 $\text{precision} \leftarrow \frac{TP}{TP+FP}$ (if $TP + FP > 0$, else 0)

1671

 $\text{recall} \leftarrow \frac{TP}{TP+FN}$ (if $TP + FN > 0$, else 0)

1672

 $F1 \leftarrow \frac{2 \cdot \text{precision} \cdot \text{recall}}{\text{precision} + \text{recall}}$ (if $\text{precision} + \text{recall} > 0$, else 0)

1673

return $F1$

1674
 1675
 1676
 1677 **Algorithm 4** Macro Semantic F1 Score

1678 **Require:** Predicted sets $\{P_1, P_2, \dots, P_n\}$, True sets $\{T_1, T_2, \dots, T_n\}$, Similarity matrix S , Label
 1679 set \mathcal{L}
 1680 Initialize $TP_c \leftarrow 0$, $FP_c \leftarrow 0$, $FN_c \leftarrow 0$ for all $c \in \mathcal{L}$ // per-class semantic counts
 1681 Initialize $\text{support}_c \leftarrow 0$ for all $c \in \mathcal{L}$ // class frequencies
 1682 **for** $i = 1$ to n **do**
 1683 Compute forward pairs: $F_i \leftarrow \{(p, \arg \max_{t \in T_i} S_{tp}) : p \in P_i\}$
 1684 Compute reverse pairs: $R_i \leftarrow \{(t, \arg \max_{p \in P_i} S_{tp}) : t \in T_i\}$
 1685 **for** each class $c \in \mathcal{L}$ **do**
 1686 **if** $c \in T_i$ **then**
 1687 $\text{support}_c \leftarrow \text{support}_c + 1$
 1688 **end if** // Update semantic true positives
 1689 **if** $c \in P_i$ and c has forward match $t^* \in T_i$ **then**
 1690 $TP_c \leftarrow TP_c + S_{t^*c}$
 1691 **end if** // Update semantic false positives
 1692 **if** $c \in P_i$ **then**
 1693 **if** c has forward match $t^* \in T_i$ **then**
 1694 $FP_c \leftarrow FP_c + (1 - S_{t^*c})$
 1695 **else**
 1696 $FP_c \leftarrow FP_c + 1$
 1697 **end if**
 1698 **end if** // Update semantic false negatives
 1699 **if** $c \in T_i$ **then**
 1700 **if** c has reverse match $p^* \in P_i$ **then**
 1701 $FN_c \leftarrow FN_c + (1 - S_{cp^*})$
 1702 **else**
 1703 $FN_c \leftarrow FN_c + 1$
 1704 **end if**
 1705 **end if**
 1706 **end for**
 1707 **end for** // Compute per-class F1 scores
 1708 **for** each class $c \in \mathcal{L}$ **do**
 1709 $\text{precision}_c \leftarrow \frac{TP_c}{TP_c + FP_c}$ (if $TP_c + FP_c > 0$, else 0)
 1710 $\text{recall}_c \leftarrow \frac{TP_c}{TP_c + FN_c}$ (if $TP_c + FN_c > 0$, else 0)
 1711 $F1_c \leftarrow \frac{2 \cdot \text{precision}_c \cdot \text{recall}_c}{\text{precision}_c + \text{recall}_c}$ (if $\text{precision}_c + \text{recall}_c > 0$, else 0)
 1712 **end for** // Return macro average or weighted average
 1713 **if** macro averaging requested **then**
 1714 **return** $\frac{1}{|\mathcal{L}|} \sum_{c \in \mathcal{L}} F1_c$
 1715 **else**
 1716 $\text{total_support} \leftarrow \sum_{c \in \mathcal{L}} \text{support}_c$
 1717 **if** $\text{total_support} > 0$ **then**
 1718 **return** $\frac{\sum_{c \in \mathcal{L}} F1_c \cdot \text{support}_c}{\text{total_support}}$
 1719 **else**
 1720 **return** $\frac{1}{|\mathcal{L}|} \sum_{c \in \mathcal{L}} F1_c$ // fallback to macro
 1721 **end if**
 1722 **end if**

 1723
 1724
 1725
 1726
 1727

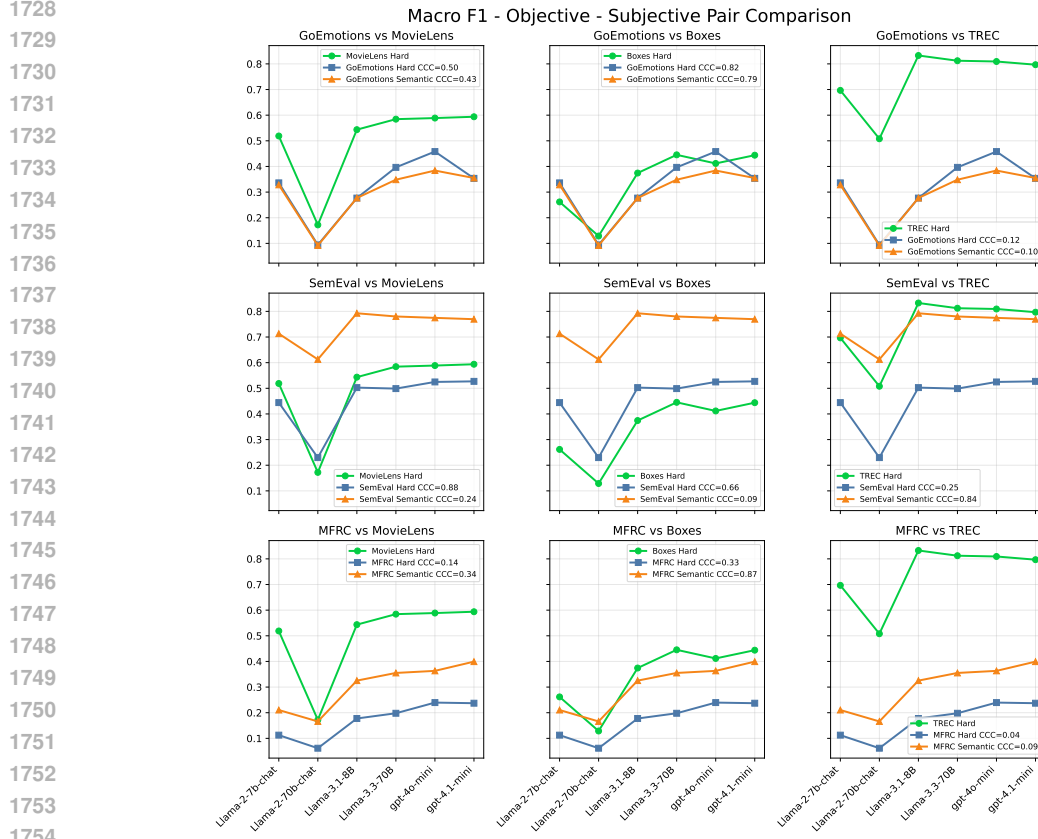


Figure 30: Semantic and hard macro F1 scores on subjective tasks correlated using CCC with hard F1 score performance in objective tasks, shown for every pair of objective-subjective dataset.

H LLM USAGE

OpenAI’s ChatGPT was used to improve the prose in the paper. Anthropic’s Claude and OpenAI’s ChatGPT were used internally as reviewers of the paper, helping us further improve the phrasing, while also suggesting experimental improvements. OpenAI’s ChatGPT and Anthropic’s Claude also assisted in the visualization of the results by providing the initial code for the plotting functions, and provided the backbone for the synthetic studies. All was manually checked and corrected by the authors.